

*Development of Polymer Based Nanocomposite Films for EMI*

*Control Applications*



**By**

**Najaf Rubab**

**(324-FBAS/MSPHY/F14)**

**Supervisor:**

**Dr. Shaista Shahzada**

Assistant Professor

Department of Physics, FBAS, IIUI

**Co-Supervisor:**

**Dr. Muhammad Raffi**

Deputy Chief Scientist

NILOP, Islamabad

**DEPARTMENT OF PHYSICS**

**FACULTY OF BASIC AND APPLIED SCIENCES**

**INTERNATIONAL ISLAMIC UNIVERSITY**

**ISLAMABAD**





*Development of Polymer Based Nanocomposite Films for EMI*

*Control Applications*



**By**

**Najaf Rubab**

**(324-FBAS/MSPHY/F14)**

**Supervisor:**

**Dr. Shaista Shahzada**

Assistant Professor

Department of Physics, FBAS, IIUI

**Co-Supervisor:**

**Dr. Muhammad Raffi**

Deputy Chief Scientist

NILOP, Islamabad

**DEPARTMENT OF PHYSICS**

**FACULTY OF BASIC AND APPLIED SCIENCES**

**INTERNATIONAL ISLAMIC UNIVERSITY**

**ISLAMABAD**





Accession No ~~TH17289~~

MS  
620.5  
NAD

Nanotechnology  
Electromagnetic spectrum  
X-ray diffraction.

*In the name of Allah, the almighty most  
Merciful and the most beneficent*



**INTERNATIONAL ISLAMIC UNIVERSITY, ISLAMABAD**

**FACULTY OF BASIC AND APPLIED SCIENCES**

**DEPARTMENT OF PHYSICS**

***Development of Polymer Based Nanocomposite Films for***

***EMI Control Applications***


**By**

**Najaf Rubab**

**(Registration No. 324-FBAS/MSPHY/F14)**

A thesis submitted to  
**Department of Physic**  
for the award of the  
degree of

**MS Physics**

  
**DR. Shamaila Sajjad**  
Chairperson  
Department of Physics (FC, FBAS)  
International Islamic University  
Islamabad

Signature: \_\_\_\_\_

(Chairperson, Department of Physics)



Signature: \_\_\_\_\_

(Dean FBAS, IIU, Islamabad)

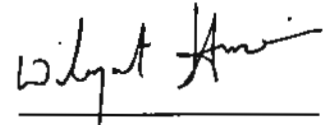
**INTERNATIONAL ISLAMIC UNIVERSITY, ISLAMABAD**  
**FACULTY OF BASIC AND APPLIED SCIENCES**  
**DEPARTMENT OF PHYSICS**

**FINAL APPROVAL**

It is certified that the work presented in this thesis entitled "*Development of Polymer Based Nanocomposite Films for EMI Control Applications*" by Najaf Rubab bearing Registration No. 324-FBAS/MSPHY/F14 is of sufficient standard in scope and quality for the award of degree of MS Physics from the International Islamic University, Islamabad.

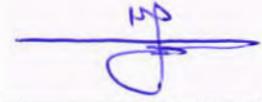
**COMMITTEE**

**External Examiner**



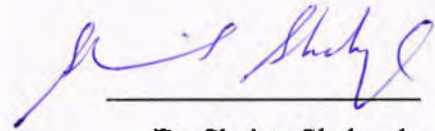
Dr. Syed Wilayat Husain  
Professor, Department of Materials Science and Engineering  
Institute of Space Technology, Islamabad

**Internal Examiner**



Dr. Naeem Ahmed  
Assistant Professor  
Department of Physics, FBAS, IIUI

**Supervisor**



Dr. Shaista Shahzada  
Assistant Professor  
Department of Physics, FBAS, IIUI

**Co-supervisor**



Dr. Muhammad Raffi  
Deputy Chief Scientist  
NILOP, Islamabad

A thesis submitted to  
**Department of Physics**  
International Islamic University, Islamabad, Pakistan  
As a partial fulfillment of requirements for the award of the degree of  
**MS Physics**

## Declaration of Originality

I, Najaf Rubab, Registration No. 324-FBAS/MSPHY/F14 hereby declare that the work presented in the following thesis is my own effort, except where otherwise acknowledged and that the thesis is my own composition. No part of the thesis has been previously presented for any other degree. If the violation of HEC rules on research has occurred, I shall be liable to the disciplinary action under the plagiarism rules of Higher Education Commission (HEC), Pakistan.

Date: 01-02-2017

Signature: Najaf Rubab

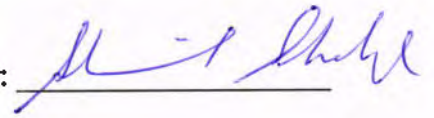
Najaf Rubab



# Certificate

It is certified that Miss Najaf Rubab, Registration No. 324-FBAS/MSPHY/F14 has carried out the research work related to this thesis entitled "*Development of Polymer Based Nanocomposite Films for EMI Control Applications*" under our supervision. This work fulfills all the requirements for the award of MS Physics.

Supervisor: \_\_\_\_\_



(Dr. Shaista Shahzada)

Co-Supervisor: \_\_\_\_\_



(Dr. Muhammad Raffi)

*Dedicated*

*To:*

*My Parents & Teachers*

*For their heartfelt supports*

## Acknowledgement

In the name of Allah, the Most Gracious, the Most Merciful.

First and foremost, I would like to thank my Creator for giving me a still functioning body and mind in order to live life and learn, and particularly to work on my dissertation project, hereby completing my Master's studies.

I must give my high, respectful gratitude to my supervisor, **Dr. Shaista Shahzada** and co-supervisor **Dr. Muhammad Raffi**, for their guidance, supervision and help throughout this research project. I have learned a lot throughout this research project, with many challenging yet valuable experiences in order to complete this task. My endless thanks to both of Dr. Shaista Shahzada and Dr. Muhammad Raffi for giving me the opportunity to explore new dimensions of knowledge, as well as for providing me valuable guidance and advice in order to improve myself as a better professional person.

I am also grateful to the Head of Department of Physics, Dr. Shumaila Sajjad for providing me facilities where and whenever it was needed.

I would like to acknowledge the support of Dr. Mushtaq Ahmed, Director who has been kind enough to extend facilitation, Dr. Arshad Mehmood, Head of Materials division, Dr. Zahid Ali, and Staff of the Materials Lab for providing me opportunity to avail the facilities required to complete my research in this prestigious institute. I appreciate the learning environment provided to me.

I am thankful to Dr. Izhar Ahmed and Dr. Sabhi-u-din Khan at NILOP for knowledgeable and fruitful discussions during execution of my

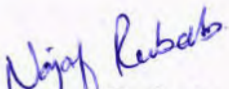


experimental work. Their scientific advice and suggestions have always been extremely helpful for the fulfillment of the data analysis and write up.

My sincere gratitude for Dr. Tanveer Ashraf, Ms. Uzma and Dr. Izhar Ahmed for giving me access to the lab facilities of electrical characterization and terahertz spectroscopy at NILOP. I am especially grateful to Dr. Mazhar Mahmood (PIEAS) and Tahir Mahmood (IST) for giving access to the materials characterization facilities.

I would like to thank my dear friends and colleagues; it has been great to know all of you during my time in MS. Finally, a great acclamation goes to my Father, whose love, prayers, encouragement, and support gave me the strength to complete this research work successfully and also for their unconditional help.

I would like to express my eternal appreciation towards my parents and family members who have always been there for me no matter where I am, for their unconditional supports and patience. Thank you for being ever so understanding and supportive.

  
**Najaf Rubab**

**IIU, Islamabad**

# Contents:

Acknowledgement.....	
List of Tables: .....	vi
List of Nomenclature: .....	vii
Abstract:.....	ix
<i>CHAPTER 1</i> .....	<b>1</b>
1. Introduction: .....	1
1.1 Objectives:.....	4
<i>CHAPTER 2</i> .....	<b>5</b>
2. EMI Shielding Theory and Literature Review: .....	5
2.1.1 Electromagnetic spectrum:.....	6
2.1.2 Radio Frequency Spectrum:.....	7
2.1.3 Tera-Hertz Band Spectrum.....	8
2.2 Elements of EMI: .....	9
2.2.1 Source: .....	10
2.2.2 Path: .....	10
2.2.3 Receiver: .....	11
2.3 Electromagnetic Compatibility (EMC): .....	12
2.4 EMC Regulations: .....	12
2.4.1 EMC Regulatory Bodies:.....	13
2.4.1.1 Federal Communication Commission (FCC):.....	13
2.4.1.2 Verband Deutscher Elektrotechniker (VDE):.....	14
2.4.1.3 Voluntary Control Council For Interference (VCCI): .....	14
2.4.1.4 Comite International Special Des Perturbations Radioelectrique (CISPR):	14
2.4.1.5 International Electrotechnical Commission (IEC):.....	14

2.4.1.6	Comite' Europeen de Normalisation Electro- technique that means European Standardization Committee for Electrical Products (CENELEC): .....	14
2.4.1.7	Military EMC Standards: .....	14
2.5	EMI Countermeasures:.....	15
2.5.1	Source Elimination: .....	15
2.5.2	Grounding: .....	15
2.5.3	Filters: .....	16
2.5.4	Shielding: .....	16
2.6	Shielding Requirements: .....	16
2.6.1	Mechanism and Materials used for shielding: .....	17
2.6.2	Polymer Nanocomposites for EMI Control Application: .....	20
<i>CHAPTER 3</i> .....		27
3.	Synthesis and Characterization Techniques: .....	27
3.1	Synthesis Process: .....	27
3.1.1	Solvent Evaporation:.....	27
3.2	Characterizations Techniques: .....	28
3.2.1	X-ray diffraction: .....	28
3.2.1.1	X-Ray Diffractometer: .....	30
3.2.2	Scanning Electron Microscopy: .....	31
3.2.3	Energy Dispersive X-ray Spectroscopy:.....	33
3.2.4	Fourier Transform Infrared Spectrometer:.....	34
3.2.6	Terahertz Time Domain Spectroscopy: .....	37
<i>CHAPTER 4</i> .....		40
4	Materials and Methodology:.....	40
4.1	Materials:.....	40
4.2	Method: .....	40



4.2.1	Weight percentage: .....	41
4.2.2	Sample preparation: .....	42
4.2.3	Flowchart of Experimental Work: .....	44
<i>CHAPTER 5</i> .....		<b>45</b>
5	Results and Discussion: .....	<b>45</b>
5.1	Optimization of Parameters:.....	<b>45</b>
5.1.1	Hydrophobicity: .....	45
5.1.2	Evaporation time:.....	45
5.1.3	Center to edge thickness variation: .....	46
5.1.4	Pinholes:.....	46
5.1.5	Film stiction: .....	47
5.1.6	Optimized samples:.....	48
5.2	Results: .....	<b>49</b>
5.2.1	XRD Analysis: .....	49
5.2.2	FTIR Analysis:.....	50
5.2.3	FESEM Analysis:.....	51
5.2.4	EDX Analysis: .....	56
5.2.5	Four Point Probing:.....	57
5.2.6	THz-TDS Analysis: .....	60
6	Conclusion & Future outlook: .....	<b>65</b>
6.1	Conclusions: .....	<b>65</b>
	Future Recommendations: .....	<b>66</b>
	<i>References:</i> .....	<b>68</b>

## List of Figures:

Figure 2-1: Spectrum of EMI pollution .....	6
Figure 2-2: Electromagnetic Spectrum .....	6
Figure 2-3: Summary of EM noise sources and level(Bigg 1984). .....	7
Figure 2-4: Basic Elements of EMI [13].....	10
Figure 2-5: Basic Mechanism of EMI Shielding(White 1971).....	18
Figure 3-1: Schematics of solvent evaporation.....	28
Figure 3-2: Bragg's diffraction from crystal planes. ....	29
Figure 3-3: Geometric arrangement of X-Ray Diffractometer (Leng 2009). ....	30
Figure 3-4: Working principle of SEM.....	31
Figure 3-5: Schematic diagram of SEM(M Joshi, A Bhattacharyya et al. 2008). ....	33
Figure 3-6: Schematics of FTIR Spectrometer (Downes and Elfick 2010).....	34
Figure 3-7: Four probe method for measuring resistivity.....	36
Figure 3-8: Four probe method for measuring resistivity.....	37
Figure 3-9: Schematics of THz-TDS Technique. ....	38
Figure 5-1: Thickness Variation. ....	46
Figure 5-2: Adhesion issue of Composites .....	47
Figure 5-3: Optimized Samples. ....	48
Figure 5-4: XRD patterns of PMMA composite film with different loadings of CNFs (S1) reference sample (S2) 2.5wt% loading of CNFs (S3) 5wt% loading of CNFs (S4) 7.5wt% loading of CNFs (S5) 10wt% loading of CNFs (S6) 12.5wt% loading of CNFs .....	49

Figure 5-5: FTIR spectra of Samples.....	51
Figure 5-6: EDX shows the characteristics of CNFs dispersed in PMMA polymer matrix.....	56
Figure 5-7: EDX shows the characteristics of CNFs dispersed in PMMA polymer matrix.....	57
Figure 5-8: Variation of electrical conductivity with different loading of CNFs .....	58
Figure 5-9: Variation of electrical conductivity with different loading of CNFs.....	59
Figure 5-10: THz electric field amplitude in time domain of reference sample and polymer nanocomposite with different loading of CNFs.....	60
Figure 5-11: Shielding Effectiveness in THz frequency range 0.2-1.2 THz .....	61
Figure 5-13: SE at two different probing frequencies 0.3 THz & 0.9 THz .....	62
Figure 5-14: Increase of Shielding effectiveness in THz Frequency range.....	63
Figure 5-15: Electrical Conductivity VS. Shielding Effectiveness .....	64



## **List of Tables:**

**Table 2-1: Shielding Effectiveness and % Attenuation .....17**

**Table 4-1: Solution compositions employed for synthesis of polymer-CNF composites.....42**

## List of Nomenclature:

$\sigma_r$	Electrical Conductivity
$\sigma$	Electrical Conductivity
$\mu_r$	Permeability
$\mu$	Magnetic Permeability
$\epsilon$	Permittivity
$\delta$	Skin Depth
$\theta$	Bragg's angle
$\Lambda$	Wavelength
ABS	Acrylonitrile-butadiene-styrene
CNFs	Carbon nanofibers
CNTs	Carbon nanotubes
dB	Unit of shielding effectiveness of the material
DMA	dimethylacetamide
DMF	Dimethylformamide
EM	Electromagnetic
EDS	Electrostatic Discharge
EMI	Electromagnetic Interferences
f	Frequency
FFT	Fast Fourier Transform
Fs	Femtosecond
LDPE	Low Density Polyethylene
MWCNTs	Multi Walled Carbon Nanotubes
PANI	Polyaniline

PC	Polycarbonate
PCL	Poly(caprolactone)
PE	Poly(ethylene)
PEEK	Poly(ether ether ketone)
PET	Poly(ethylene terephthalate)
PEVA	Poly(ethylene-vinyl acetate)
PLLA	Poly(L-lactide)
PMMA	Poly(ethylene methyl acrylate)
PMTT	Poly (trimethylene terephthalate)
PP	Poly(propylene)
PS	Polystyrene
PUR	Polyurethane
PVDF	Polyvinylidene fluoride
PVP	Polyvinylpyrrolidone
RFI	Radio Frequency Interference
SE	Shielding Effectiveness
SEM	Scanning Electron Microscopy
THz-TDS	Terahertz Time Domain Spectroscopy
XRD	X-ray Diffraction

## **Abstract:**

Electromagnetic (EM) wave absorbing materials have attracted significant attention recently because of the expanded EM interference problems. Performance of EM absorption materials depends on both their dielectric and magnetic loss properties. However, the existing microwave absorbing materials have several drawbacks, such as being heavy, less durable and effective only over fixed frequency bands. The current challenges for development of next generation EM absorbers are to tailor novel lightweight smart materials with wide absorption frequency, high thermal stability and resistance to oxidation. Polymer nanocomposites possess a unique combination of electrical, thermal, dielectric, magnetic and mechanical properties which are useful for suppression of electromagnetic noises. These are considered promising smart materials for microwave applications due to their potential for miniaturization, tunability and realization of low-loss magneto-dielectric materials with flexibility to tailor permittivity and permeability. In this work, nanocomposite films of PMMA loaded with 0.00-12.50wt% of carbon nanofibers (CNFs) were designed and prepared by solvent evaporation method used as tunable electromagnetic attenuation and interference shields. Stable and uniform PMMA solutions were prepared in Acetone by magnetic stirring, CNFs were dispersed using a probe sonicator. These dispersions were subsequently poured into PYREX petri dishes moulds of 2 inches for evaporation of solvent, firstly by placing them in lab oven and then at room temperatures for 48 hours to get stable and uniform films of PMMA and CNFs. The structure, morphology and thickness of these films were characterized by XRD, FTIR and FESEM. These films were observed to have a nice entanglement of CNFs, bonded with polymer matrix with uniform thickness estimated by field emission scanning electron microscopy. Electrical characteristics and Shielding effectiveness and of these samples were measured by four probe method and terahertz time domain spectroscopy (TDS) in the frequency range of 0.2THz-1.2THz respectively. A well-ordered trend in conductivity of these films has been observed as a function of CNF loadings. A systematic increasing trend in the shielding effectiveness has been observed by the TDS, but a maximum SE of 56 dB has been evaluated in the samples having 12.50wt% loading of CNFs. These polymer nanocomposite film samples are good runners as flexible shielding materials in terahertz frequencies.

## CHAPTER 1

### 1. Introduction:

Electromagnetic interference (EMI) shielding refers to the reflection and/or adsorption of electromagnetic radiation by a material, which thereby acts as a shield against the penetration of the radiation through the shield. EMI shielding of both electronics and electrical sources is needed and is increasingly required by industry, commercial, domestic, defense product, designers and manufacturers around the world like electromagnetic radiation, generally at high frequencies (e.g. radio waves, such as those emanating from cellular phones) tend to interfere with electronics (e.g. computers). The significance of EMI shielding has been highlighted with the demand of today's society on the reliability of electronics and the rapid growth of radio frequency radiation sources. The expansion of electronic devices and instrumentations in domestic, commercial, industrial, electronic appliance, healthcare, home appliances and defense areas generate a pollution defilement referred to as *Electromagnetic Interference (EMI)*. As a result of EMI, temporary disruption of normal functionality or total breakdown of semiconductor base equipment occurs caused by the interference between commercial equipment, process machines, consumer products and other devices may cause. The distress through wireless communication, mechanization and process control may result into loss of reliable performance, energy, money, time or even human life. Induced currents by electric and magnetic fields, originating through a nearby broad range of electric circuitry are other factors that also causing electromagnetic interference. As a result, shielding and hardening devices ought to be designed to mitigate the interfering contents from specious electromagnetic clamors [1-3]. The unwanted influence of EMI on the electronic efficiency and human health has triggered search for appropriate shielding methodologies and materials. Wireless communication, radar navigation, local area networks and many other uses of electromagnetic signals are the rapid advancements result into highlighting the significance of EMI shielding [4]. An EMI shield should have a higher conductance, therefore metals, such as copper, aluminum, steel, etc., are the most prevalent materials employed for EMI shielding applications. Since metallic



shielding materials have disadvantages of physical stiffness, prone to corrosion and heavy in weight [5]. Additionally, the shielding mechanism of metals is based on the reflection of electromagnetic radiation from their surfaces which limit their utilization where absorption is primarily essential for blocking the radiated electromagnetic energy e.g. in stealth technology [6]. In the current market, consumers are requiring lighter in weight and more compact electronic devices with enhanced efficiency and layout choices. Appropriately, conductive filler/ polymer composite recently have got attraction to be utilized for electronic devices due to their exceptional properties such as light weight, tunable electrical conductivity, low cost, processability and corrosion resistance etc. Because of the tunable electrical conductivity, polymer nanocomposite are being used and further explored for a wide range of applications like charge storage devices, electrostatic discharge (EDS) safety, antistatic dissipation and EMI shielding[7, 8].

This Master of Science (MS) thesis aims to provide a systematic study on the synthesis and characterization of PMMA/CNFs based nanocomposite for EMI shielding applications. Therefore, it is integrated into the following chapters.

**Chapter 1** gives the overview and motivation of this research project. The overall layout and objectives of this dissertation are also presented.

**Chapter 2** provides the literature review on EMI generation, transmission, coupling, effects and mitigation strategies. Specifically, EMI frequency spectrum and shielding mechanism of various metallic and non-conducting materials have been described. This chapter has briefly outlined the importance of polymers and their nanocomposites being explored, studied and developed for EMI shielding applications.

**Chapter 3** describes the solvent casting method and experimental techniques used for structural, morphological and electrical characterization of the synthesized nanocomposites. Characterization techniques determine and evaluate the quality of developed nanocomposite materials. The techniques that have been used in this research work include X-ray diffraction (XRD), Fourier Transform Infrared spectroscopy (FTIR) and Scanning electron microscopy (SEM) to determine the structural and morphological character of the nanocomposite films. Four Point

Probing was carried out to determine the electrical conductivity of the developed films and Tera-Hertz Time Domain Spectroscopy was used to evaluate shielding effectiveness in Tera-Hertz region whereas S-parameters were used to analyze the shielding effectiveness in X-band.

**Chapter 4** outlines the polymers, CNFs, solvents, equipment, protocols and experimental set-up used to prepare the thin film samples. A detailed descriptions of the basic working principle are presented and discussed in this chapter.

**Chapter 5** presents the process optimization and results and discussions of experimental studies carried out on the synthesis and characterization of polymer/CNFs nanocomposite films developed by solvent evaporation.

**Chapter 6** summarizes the important results and outcomes of the research work, as well as, give an outlook for the future research direction in this exciting research field. This work will expand the current work on EMI shielding application using polymers as a matrix and CNFs/ CNTs as filler, which may prove to be useful for enhancing the shielding effectiveness by varying the fillers loading.

## **1.1 Objectives:**

The work presented in this dissertation is aimed to develop and characterize the lightweight, flexible and volume-efficient polymer based nanocomposite films loaded with a range of CNFs to make it a conductive material that can be used for EMI shielding by absorbing the radiated EM energy in Terahertz range.

## CHAPTER 2

### 2. Shielding Theory and Literature Review

#### 2.1 Electromagnetic Interference

The electromagnetic interference (EMI) of one particular system on another part of itself or other system in the vicinity has become known since work on electrical systems started about a century ago. During the Second World War, use of electronic devices, primarily radios, navigational devices and radars accelerated.

Instances of interference between radios and navigational devices on aircraft began to increase [9]. It is only after the Second World War that this problem has become of general interest. These problems were solved by reassigning the transmitting frequencies in the uncrowded spectrum because the density of the electronics was far less than what it is today. Most significant increase in the interference problem occurred with the invention of high density semiconductor based electronic components like transistors, integrated circuits, microprocessors, devices and systems during 50's, 60's and 70's.

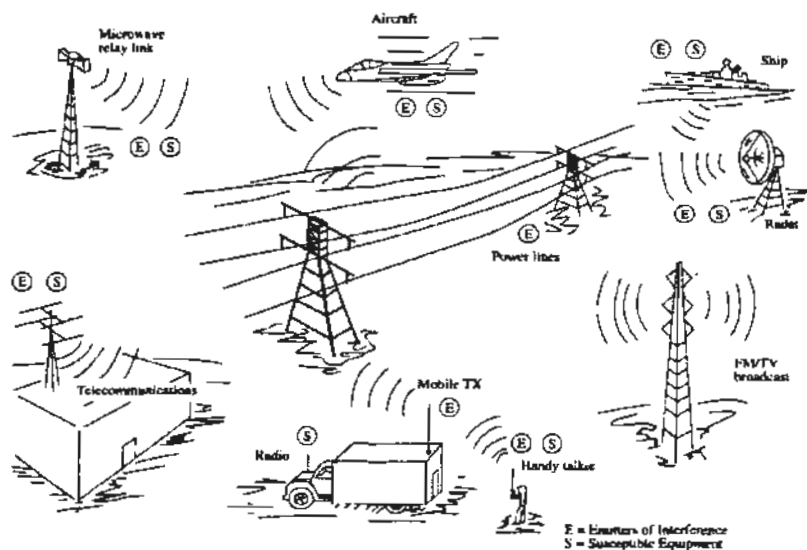


Figure 2-1: Spectrum of EMI pollution

The frequency spectrum also became more crowded due to the increased demand and utilization for voice and data communication. Cellular telecommunication cannot function satisfactorily in electromagnetically polluted environment. Digital signal processing and computing has brought the emphasis on electromagnetic compatibility (EMC) to the forefront [10]. The evidence suggests that this issue has become a major environmental concern in the recent years as the use of electronic equipment has spread throughout every aspect of our lives.

### 2.1.1 Electromagnetic spectrum

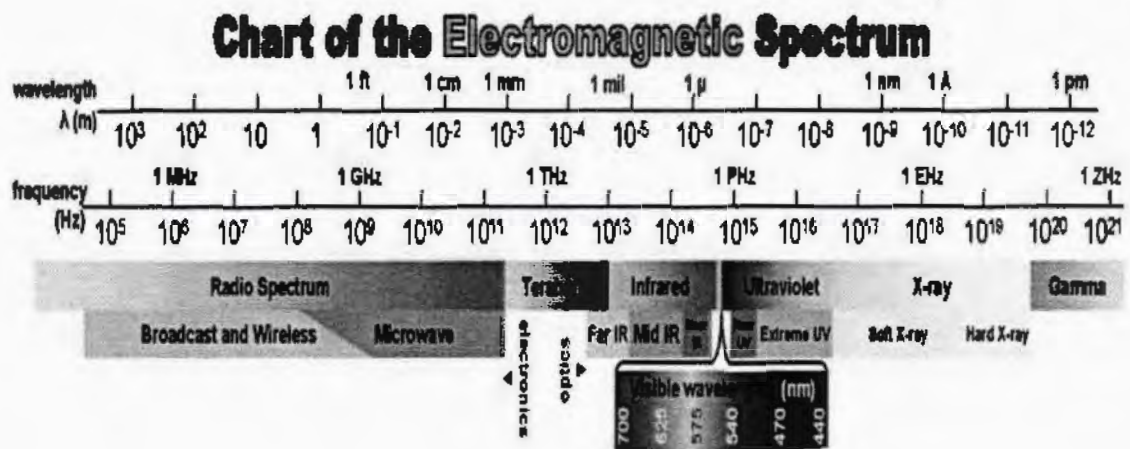


Figure 2-2: Electromagnetic Spectrum [9].

The above figure describes the several forms of electromagnetic interference source that differ from one another by their wavelength or frequency.

### 2.1.2 Radio Frequency Spectrum

Unlike the other environmental pollutions like air, water, etc. there is one and the only frequency spectrum for use by all mankind. There is no other substitute of the spectrum. Therefore, the rate of increasing use of intentional and unintentional electronic devices, wireless data communication cause noise and crowded the frequency spectrum.

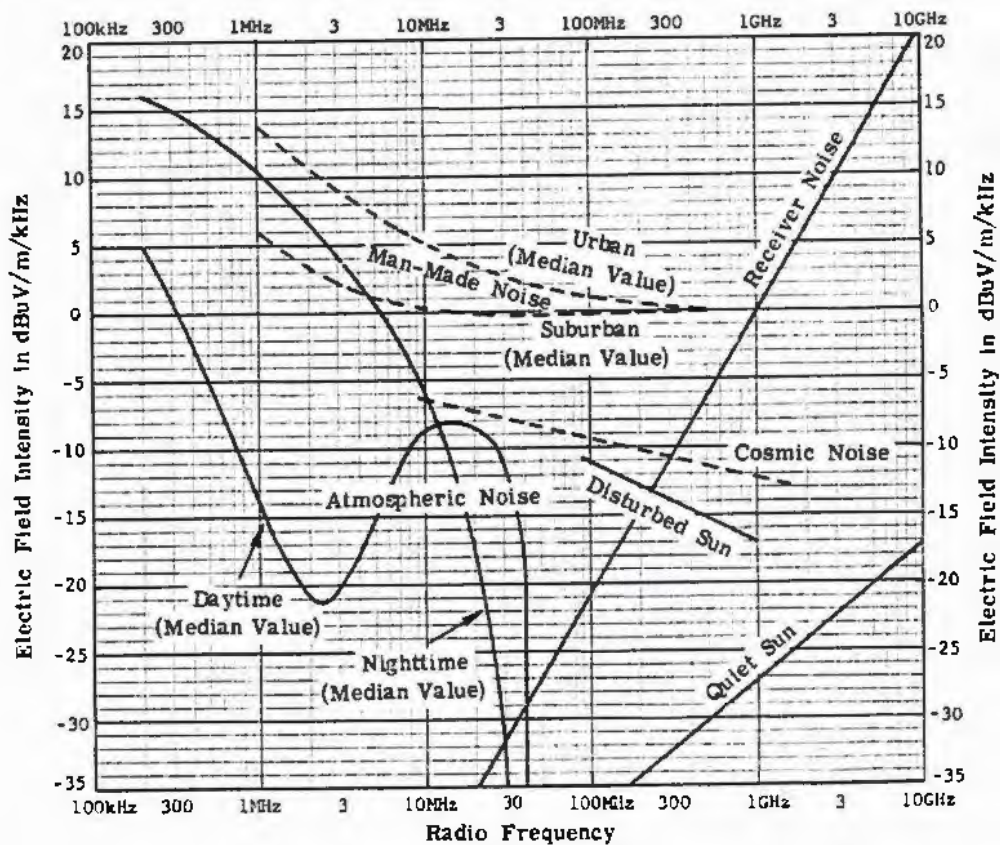


Figure 2-3: Summary of EM noise sources and level [10].

Figure 2-3 describe many sources of EMI in the frequency spectrum spread from 100 KHz – 10GHz. All the communication sources, including electronic, industrial, scientific and man-made noise are grouped in under the urban and suburban categories. Natural EM sources are also responsible for pollution in spectrum primarily placed in the atmospheric region ~10MHz. This kind of specific noise is mostly generated by lightning or thunderstorms. Cosmic is also a natural source of noise that originates from galaxy. This figure also shows solar radiations; both quiet and disturbed.

### 2.1.3 EMI Issues, Challenges and Mitigation:

As previously mentioned, that the primary shielding mechanism by using conducting materials is reflection. The theoretical shielding equations suggest that reflection can be achieved by using highly conducting materials with low values of permittivity/permeability. Therefore, addition of conducting fillers, that can form percolation network in the host polymer matrix, seems to be the solution for



inducing electrical conductivity in the nanocomposites. However, the incorporation of nanomaterial within polymer matrix is not a straight forward task because of the ultrahigh surface area and agglomeration tendencies. This often resulted in failure to efficiently transform the nanoscopic properties of these fillers into macroscopic properties of resultant nanocomposites and inability to grasp their full potential. Therefore, handling and dispersion of nanofillers is the biggest challenge not only for nanocomposites technologies but for nanoscience as a whole. Nevertheless, so much progress has already been made in the development of polymer based nanocomposites and the same will be discussed in the next section. For convenience of understanding, fillers have been classified into three broad categories: metal or carbon, conducting polymer, dielectric/magnetic functionality based [11].

#### 2.1.4 Tera-Hertz Frequency Band Spectrum

The Tera-Hertz Band is the spectral band that spans the frequencies between 0.1 THz and 10 THz. While the frequency regions immediately below and above this band (the microwaves and the far infrared, respectively) have been extensively investigated, this is still one of the least-explored frequency bands for communication. The THz band offers a much larger band width, which ranges from tens of GHz upto several THz depending on the transmission distance [11].

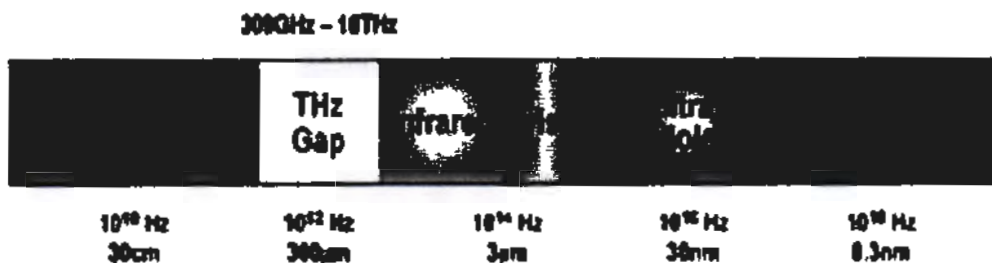


*Figure 2-4 Electromagnetic spectrum showing the THz band gap [12]*

To characterize the reflection, scattering and diffraction coefficients at THz band frequencies, the properties of building materials have been measured up to 1 THz for

communal materials. Tera-Hertz Band communication will report the spectrum dearth and capacity limits of current wireless systems, and enable an excess of applications, such as ultra-fast massive data transfers among nearby devices, or high-definition video conferencing among mobile personal devices in small cells. THz band will also enable innovative networking standards at the nanoscale, such as Wireless NanoSensor Networks and the Internet of Nano-Things [11].

## 2.2 Elements of EMI:

**Electromagnetic Interference**, EMI requires three basic constituents.

### 1- SOURCE

### 2- PATH

### 3-RECEIVER

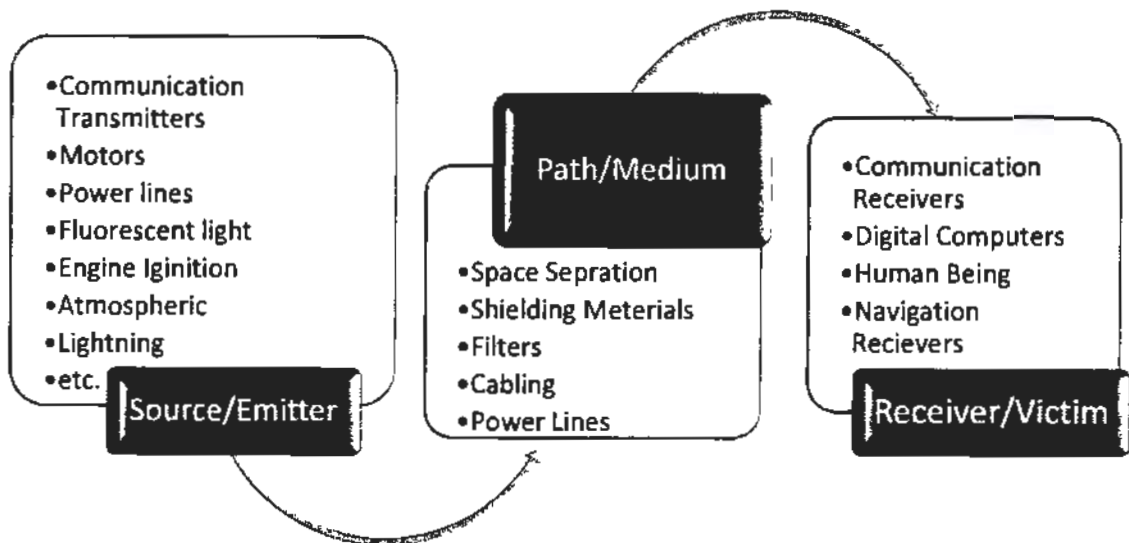


*Figure 2-5: Basic Elements of EMI [13]*

The **Figure 2-4** illustrates the three basic elements that are responsible for EMI. They consist of electrical noise source, coupling path and receiver. If any of the three is missing, EMI does not occur. The potential for EMI exists even in the absence of a receiver [11].

**2.2.1 Source:**

An EMI noise source is any system that is generating unwanted electromagnetic signals. There are basically three categories of EMI noise sources, intrinsic, natural and man-made [12].

**2.2.2 Path:**

There are basically two EMI propagation paths, radiated and conducted. Transfer of electromagnetic energy is further divided into four sub groups: *radiated emission, radiated susceptibility, and conducted emission, conducted susceptibility*. Radiated EMI is transmitted through free space as (Radio Frequency) RF energy. Conducted EMI is transmitted along cables used to power or interconnect the device in question. Interfering signals may also follow both the paths. EMI energy can couple with electronic systems through any conducting medium like power lines, antennas, utility lines, slits and slots in casings etc. The arrangement of printed circuit board (PCB) lands and cabling inside the systems are also very important aspects. EMI energy thus reaches to the constituent component results in permanent damage in which junction breakdown occurs because of excess flow of current and heat. The dominant coupling modes are investigated for vulnerability analysis and EMI solutions [12].

**2.2.3 Receiver**

Receivers are all those victim electronic systems or sub systems, which are effected by EMI. An electronic system is designed and developed to function in a specific frequency range and electromagnetic environment. Electromagnetic noise from intentional and/ or unintentional sources couples with the receiver and causes damage to the system or degrade performance of the system (receiver).

**Classification of Products**

1. Domestic
2. Industrial
3. Scientific
4. Medical

## 5. Military

### **2.3 Electromagnetic Compatibility (EMC)**

Electromagnetic Compatibility (EMC) is the capability of a device, equipment or system to perform suitably in its electromagnetic environment without introducing unendurable electromagnetic disturbances to anything in that environment.

Factors that affect electromagnetic interference vulnerability are;

- EMI environment
- System response
- System threshold and sensitivity
- System mission

### **2.4 EMC Regulations:**

There are two basic classes of EMC requirements that are executed on the electronic systems:

- ✓ Those authorized by the government agencies
- ✓ Those executed by the product manufacturers

The requirements executed by government agencies are authorized requirements and cannot be waived off. These requirements are imposed in order to control the interference produced by products. Compliance with the EMC regulations does not guarantee that the product will not cause interference but to control the amount of electromagnetic pollution that the product generates and keep it within legal limits.

Contrariwise, EMC requirements imposed by the industrialists on their products are intended to result in customer satisfaction. They are imposed for the purpose of ensuring a reliable, quality product.

## **2.4.1 EMC Regulatory Bodies:**

### **2.4.1.1 Federal Communication Commission (FCC):**

In United States of America, the Federal Communication Commission is stimulating with the parameters of radio and wire communication. The major responsibility of this body is to control interfering from and to wire and radio communication. Radio frequencies extend from 9 kHz to 3000 GHz in the range of frequencies defined by the FCC. A radio frequency device is any device that is capable of emitting radio frequency energy by radiation, conduction or other means whether intentionally or not. FCC classified digital devices possessed by class A and class B. Devices that are marketed for use in a commercial, industrial or business environment assigned to Class A digital devices. Class B digital devices are those that are marketed for use in residential environment, notwithstanding their use in a commercial industrial or business environment. The class B limits are more stringent than the class A. Interference from the stratagem in an industrial environment can be further readily modified than in residential environment where the interference source and susceptible device are likely to be in more immediacy.

### **2.4.1.2 Verband Deutscher Elektrotechniker (VDE):**

This regulation is imposed by the German government. The general requirements in this regulation are quite similar to the FCC requirements. But the frequency ranges and limits levels are slightly different.

### **2.4.1.3 Voluntary Control Council for Interference (VCCI):**

This council is working in Japan to regulate and control the electromagnetic interference.



**2.4.1.4 CISPR** (*Comite International Special Des Perturbations Radioelectrique*):

**2.4.1.5 IEC** (*International Electrotechnical Commission*):

**2.4.1.6 CENELEC** (*Comite` European de Normalisation Electro- technique that means European Standardization Committee for Electrical Products*):

These are the regulations imposed by the European Union (EC) to their products to control the electromagnetic interference. These regulations are applied uniformly on the regular and associated member countries of EC.

#### **2.4.1.7 Military EMC Standards**

EMC regulations for military electronic hardware are issued by the defense organizations like United States Department of Defense in United States of America. MIL- STD- 461 and MIL- STD-462 are formulated by United States Department of Defense, these describe the limits that must be met and also the procedures for making tests. These standards are more stringent than the commercial regulations. These standards cover both emission and susceptibility of the electronic system in question and the frequency range from 30 Hz to 40 GHz. The Military Specification is a comprehensive document and must be complied by the military hardware manufacturing industry.

## **2.5 EMI Countermeasures**

There are various probable countermeasures in order to counter the consequences of interferences using electronic and communication systems. The corrective steps could be very sophisticated if the interference is caused by multiple sources. Here are some of technique used to reduce or eliminate the effect of EMI: [12]

### **2.5.1 Source Elimination:**

A simple yet effective way to eliminate interference is by detection and eradication of source that is responsible of interference. Theoretically, this signifies probably the effecting of any measure, but practiced in most of circumstances where source required to be to operate periodically, can't eliminate the source [12].

### **2.5.2 Grounding:**

The grounding point symbolizes a one common reference point for a gadget or number of equipment that operates to ensure the protection of the devices and user, and its effects offer some protection to interference. Particular transmission and electronic devices need sufficient grounding to ensure appropriate operation. The conductor used to grounding the equipments, is the quick access to prevent from coupling and transfer energy to the device [12].

### **2.5.3 Filters:**

The use of band pass/ stop filters enable to feed desired frequencies to the specific devices, while rejecting frequencies which are not in the range of the filter. For example: installation of low-pass, band-pass, high-pass filters [12].

### **2.5.4 Shielding:**

An effective method accustomed to reducing, mitigating and sometimes eradicate EMI, is to properly shield circuits, components and systems against coupling and interaction with electromagnetic waves. Shielding requires the highly conductive material that entirely encloses the devices or circuitry to prevent from interference [12].

## **2.6 Shielding Requirement:**

The basic requirement of materials used for shielding is, the surface of material should be electrical conductive enough to protect the material or equipment from outer field. Usually this only refers to the electric field, while the magnetic field involves totally different mitigation procedure, such as use of thicker material and sealed packaging, etc.

Though the conductivity is important, but not sufficient enough to give attenuation against noise signal. Bigg's statement, to achieve 30dB attenuation, material should possess resistivity of 2 ohm-cm or less [10]. It is known that 99.9% of interrupting signal can be stop at 30dB attenuation. For most of commercial and user applications 20dB -30dB attenuation works to provide good shielding. Table 2-1 shows shielding effectiveness i.e. the percentage of attenuation against the interfering signal.

Table 2-1: Shielding Effectiveness and % Attenuation

SE(dB)	Power Ratio	% Attenuation
0	1.000	0
10	10	68
20	100	99
30	1000	99.9
40	10,000	99.99
50	100,000	99.999
60	1,000,000	99.9999
70	10,000,000	99.99999

### 2.6.1 Mechanism & Materials for shielding:

Electromagnetic interference shielding describes reflection, multiple reflection, and absorption losses as the dominant mechanisms in the materials used to block undesired EM waves [13]. The coefficient of shielding material; Transmission (T), absorption (A), and reflection (R) can be represented as

$$A=1-(T+R)$$

$$\text{Where; } T = \left| \frac{E_T}{E_I} \right|^2$$

$$R = \left| \frac{E_R}{E_I} \right|^2$$

$$\text{EMI SE (dB)} = 20 \log \left| \frac{E_T}{E_I} \right|$$

Where  $E_I$ ,  $E_T$ ,  $E_R$ , Shows the incident, transmission, and reflected electromagnetic radiation respectively.

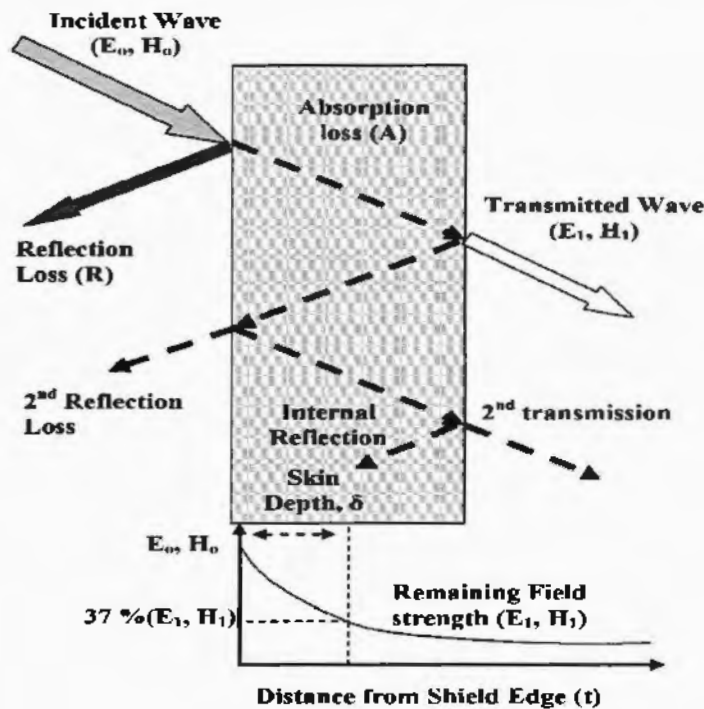


Figure 2-6: Basic Mechanism of Shielding [11]

Primarily, in metals reflection loss plays the dominant role for EMI shielding. For an efficient interaction of shielding material with the incident electromagnetic waves, reflection loss based shield materials are used that contain mobile charge carrier, electron or holes. Therefore the shield, usually conducts however a very high conductivity isn't essential for shielding [14]. Reflection loss can be expressed as a function of ratio;

$$R = \sigma_r / \mu_r$$

where  $\sigma_r$  is the electrical conductivity relative to copper and  $\mu_r$  is permeability constant relative to copper [15]. Metals such as aluminum, copper, etc. are the foremost choice for the reflection based EMI shielding [16, 17]. Metals function generally by the reflection of EM waves owing to higher mobile electrons density. To make a metal coating for shielding purpose, the electroplating and vacuum deposition are used.

The absorption loss is the second pronounced mechanism that is employed for EMI shielding. The electric or magnetic dipoles emerge in the absorption based shielding materials upon coupling of EM wave. The materials with high dielectric constant or

magnetic permeability results into emergence of electric and magnetic dipoles. Absorption loss can be evaluated by the product of  $\sigma_r \mu_r$  [13, 15]. In contrast, reflection loss decreases with an increasing frequency. In case of absorption, by increasing frequency losses also increase. These losses are directly related to thickness of the shielded material. In polymer nanocomposite materials, absorption is the prime prerequisite when used for the EM shielding.

Besides reflection and absorption, multiple reflections is also one of shielding mechanism. This refers to as a reflection of waves from the surfaces or interfaces inside the shielding material. This type of mechanism requires a large surface area of material [15].

Mutually, all resultant losses caused by reflection, absorption, or multiple reflection in a material are aggregated to shielding effectiveness of the material (in dB). EM waves at the high frequencies penetrate only at the surface of conducting material that is known as skin effect. Penetration of electromagnetic waves drops exponentially with the increasing depth of the conductor (d) is known as skin depth, given as:

$$\delta = \frac{1}{\sqrt{\pi f \mu \sigma}} \quad (2.1)$$

Where;

f = frequency

$\mu$  = magnetic permeability

$\sigma$  = electrical permittivity

It is evident that skin depth is increasing with the decreasing frequency, electrical conductivity and permeability [15].

### 2.6.2 Polymer Nanocomposites for EMI Control Application:

Due to the skin effect, novelty, weight, corrosion resistance, flexibility, conductive nanocomposites got attention to be utilized as shielding materials due to the small size of the unit cell of the conductive fillers. Nanocomposites owing to distinctive combination of mechanical, electric, dielectric, magnetic, thermal properties are considered a favorable choice of effective shielding materials against EMI [18, 19]. Generally, there are two major material elements in composite, i.e. the matrix and

reinforcement inclusions. Apart from these, there is a third phase called interfacial region that contributes towards interlacing between matrix and the fillers. Interface possesses distinctive combination of attributes that are not displayed in fillers or matrix separately [20]. In polymer nanocomposites, polymers are used as matrix material owing to their excellent dielectric/ insulating properties which does not contribute in shielding, but supports in providing connectivity of filler that enhances the SE. For the tunable electrical conductivity ( $\sigma$ ) and electromagnetic characteristics including permittivity ( $\epsilon$ ) and permeability ( $\mu$ ), the multitude of filler materials have been used for making nanocomposites [21].

In 1991 by Iijima [22], since the discovery of carbon nanotubes (CNTs) and pursuing the formation of 1<sup>st</sup> polymer/ CNTs nanocomposite by Ajayan et. al. [23], researchers intrigued towards use of CNTs/ Carbon Nanofibers (CNFs) in several fields, including chemistry, material sciences, physics and electrical engineering etc. CNTs/CNFs are distinctive nanostructured materials having exceptional physical and mechanical properties [24-26]. These attributes have encouraged the researchers on making use of CNTs/ CNFs as fillers in polymer composite to acquire nano structural material having improved electrical, optical and thermal properties [27]. The choice of polymers as matrix materials is a versatile option because of their distinctive qualities such as lower density, versatility, facile processability, corrosion resistance and so on. On the other hand, for electrical and electromagnetic shielding applications, the most important prerequisite in materials is the existence of conductivity [28]. However, mostly polymers have innate electrical insulating properties that make them nearly transparent to the electromagnetic radiations. To overcome this particular shortcoming, conductive nanoparticles/ nanotubes/ nanoheads are dispersed in appropriate amount of loadings within the polymer matrix, enabling composites to absorb incident EM waves through dissipation in the conductive particles and decrease the overall reflection as well as transmission from the surface.

In the recent past, much work reportedly has been done on the development of novel EMI shielding materials using polymer/ CNTs/ CNFs based nanocomposite by adopting different methods of dispersion of CNTs/ CNFs in polymer matrices for subsequent formation of thin films for tailoring shielding effectiveness.

When researchers started work on making polymer composites for EMI shielding application, primary method that were proposed to disperse the CNTs as filler in different polymer was melting mixing. The poly(trimethylene terephthalate) (PMTT), poly(ethylene terephthalate) (PET), poly(ethylene) (PE), polycarbonate (PC), poly(propylene)(PP), poly(ethylene-vinyl acetate) (EVA), poly(ethylene methyl acrylate) (EMA), poly(ether ether ketone) (PEEK), acrylonitrile-butadiene-styrene copolymer (ABS), poly(caprolactone) (PCL) and poly(L-lactide) (PLLA) are the polymers that were used as matrix in melt mixing process [29]. Anju Gupta and Veena Choudhary have adopted melting mixing method for dispersion of MWCNTs in poly (trimethylene terephthalate) (PMTT) to make nanocomposites. They directly dispersed the MWCNTs in PMTT by varying of loadings from 0.5% to 10% (w/w). They figured out that concentration of MWCNTs in polymer was the linearly affecting the conductivity, permittivity and shielding effectiveness of composites and increase while increasing the loading of MWCNTs. Electrical percolation was achieved at 1% (w/w) MWCNTs loading, while at 10% (w/w) shielding effectiveness of 36- 42 dB was achieved in 12.4 – 18 GHz frequency range in  $t=2\text{mm}$  of composite film. It had been studied that PTT/ MWCNTs composite having 5-10% (w/w) MWCNTs may be used as effective, light-weight EMI shielding material [30].

The paper making method is also considered one of novel approaches used for EMI shielding applications. In this method, the aqueous solution cellulose fiber in the existence of a cationic fixer were used as base material and CNTs were added in it. In order to make paper product, residual water was removed by pressing and drying [29]. Masanori Imai et al. have been made CNT/cellulose composite employing a paper making method. They have concluded that at 4.8 wt% of CNTs loading in composite paper, 50dB SE have been attained in 5-10 GHz frequency range. EMI shielding effectiveness were measured by MSL method and free space method and then qualitatively matched with theoretical characteristics obtained by the simulation. CNTs/cellulose composite, featuring a much better EMI SE, can be used to reduce EM wave interference, control undesirable reflection, avoid cross talk and noise in the circuits [31].

Mi sun ban et al. have used the solvent casting technique to develop the PC nanocomposites, a  $H_2O_2$  treatment on the MWCNTs and then PC/ MWCNTs



composite by varying the loading of MWCNTs (1-7wt %). They analyzed and evaluated that the electrical, morphological and rheological properties of PC/MWCNTs composite with and without pre-treatment of  $H_2O_2$  with MWCNTs. It has been analyzed that PC/freeze-dried MWCNTs composite with treatment of  $H_2O_2$  exhibited higher conductivity than those without treatment of  $H_2O_2$ . Morphological behavior of PC/MWCNTs composites were analyzed by TEM and AFM that showed improvement upon dispersion of MWCNTs with treatment of  $H_2O_2$  in PC matrix. That showed the EMI SE of PC/freeze-dried MWCNTs composite, treated with  $H_2O_2$  was increased relative to the without  $H_2O_2$  treating MWCNTs because of the increased dispersion of MWCNTs in PC matrix.  $H_2O_2$  treated MWCNTs composite also exhibited improvement in rheological properties of composite compared to the untreated PC/MWCNTs composite [32].

Mathur et al. did comparative research on the performance of PS and PMMA nanocomposite prepared by solvent casting method. Assimilation of MWCNTs into the polymer matrixes, both PS (thermoset) and PMMA (thermoplastic) have been carried out and their electrical properties, microstructure and mechanical properties were analyzed. At various loading of MWCNTs from 1-10vol%, they analyzed electrical conductivity for the both samples and observed almost similar SE i.e. 18 dB in frequency range 8- 12 GHz at 10Vol% of loading having 0.3mm film thickness that was specifically associated with the particular conductivity of the sample [33].

For processing of nanocomposites, In situ polymerization is another widely used method which comprises of polymerizing monomer in the presence of nano fillers. This method has been employed for making polymer nanocomposites doped with polyaniline (PANI). PANI is a conducting polymer, therefore doping of CNTs in it enhances the electrical conductivity which ultimately leads to increased shielding effectiveness [29]. Yuan-Li Huang *et al.* have done comparative analysis of two techniques i.e. in situ polymerization and solvent casting. They prepared PMMA nanocomposites by in situ polymerization of MMA in dimethylacetamide (DMA). The material is then retrieved in the form of thin films upon evaporation of solvent at 120°C for 72 hr. These thin films samples exhibited higher SE in comparison to the nanocomposites made by solvent casting method (15dB vs. 10 dB at 4.76 wt%, 2-18GHz) [34].

Making polymer based CNTs nanocomposite for EMI shielding applications, the polymer emulsion have also reportedly been used[29]. Li et al. have studied EMI SE by dispersing CNTs in a solution of styrene acrylic[35] and acrylic emulsion[36]. After evaporation of solvent, particles came up with the nanocomposite having very low percolation threshold 0.58 wt% in acrylic emulsion and 0.24 wt% in styrene acrylic. A shielding effectiveness of 20dB was observed in acrylic emulsion loaded with 8wt% CNTs in 8-12GHz frequency range whereas in case of styrene acrylic emulsion, 25dB SE was achieved at 15wt% loading of CNTs in 8-12 GHz frequency range, at thickness ( $t=2\text{mm}$ ).

Ball milling is considered more particular method for making dispersions. The ball milling is process involves inserting various material to mix inside the cylindrical container. The container comprises of small ceramic or metal balls that grind the solid material into fine powder. A compression molding operation is performed after grinding to get the specific material that is used for EMI application. A.S Hoang has prepared MWCNTs/ polyurethane composites through ball-milling technique for EMI shielding. They have discovered that at low weight fraction of MWCNTs could attain a higher level of conductivity. They have archived the 20dB SE in 8.2-12.4GHz range at 22wt% loading of MWCNTs in 100 $\mu\text{m}$  thickness of composite film [37].

Solvent casting is another popular method used to make thin films of dispersion of Polymer-CNTs nanocomposite being employed for EMI shielding. This method has been used for PMMA (Polymethyl methacrylate), PVDF (Polyvinylidene fluoride), PC (Polycarbonate), PVP (Polyvinylpyrrolidone), PS (Polystyrene), PUR (Polyurethane), LDPE (Low Density Polyethylene), and lotader epoxy. This method is based on solubilization of polymer in CNTs based solution accompanied by the evaporation of the solvent [29].

The electro spinning process which is based on electrostatic forces which pulls out a jet of polymeric solution effused through a syringe under high voltage onto the conductive substrate, producing nanofibers that can be employed for EMI shielding applications [29]. Evenly sized CNT-embedded PAN nanofibers were effectively made by electrospinning method by dispersion of CNTs in PAN solution, perused by Chen et al. These samples have been analyzed for EMI shielding effectiveness in 300 MHz-3 GHz frequency range. The results indicated that the carbon fiber sheet of

thickness 150 $\mu$ m possess a significant shielding effectiveness of more than 15 dB [38].

Spray coating is one of the efficient methods of making thin films used for EMI shielding. The spray coating technique is comprised of spraying polymer/CNTs solution onto a substrate. In this method, solvents of the dispersion rapidly evaporates thus forming a composite thin film onto the substrate [29]. Y. Yang et al. have developed a novel CNTs-polystyrene foam composite intended for EMI shielding application by mean of spray coating technique. They have observed 20 dB shielding effectiveness at 7 wt% loading of CNTs in PS matrix in the x - band which shows that CNTs- Ps foam matrix can be employed at the commercial level as a shielding material for EMI applications. It has also been analyzed that at same loading CNTs-PS foam provide more effective shielding against EMI as compared to CNFs-PS foam composites [39]. Arindam das et al. have explained the synthesis and characterization of super hydrophobic, CNFs/PTFE filled polymer composite by spray coating technique, possessing higher electrical conductivity. The PMMA/PVDF polymer blend was severed as a matrix with having a good interfacial adhesion and elasticity. The conductivity of the coating have been tailored by adding different loadings of CNFs in polymer matrix. They have reported EMI SE of super hydrophobic, conductive-polymer based coatings in x-band frequency range. They have reportedly achieved SE up to 25dB in these coatings of 100 $\mu$ m thickness. Their results showed the potential of the film not just for EMI shielding applications, but also for various technologies that required excessive liquid repellency as well as higher conductivity at the same time. This synthesis approach is attractive because it enables the use of material additionally for shielding purpose, as the requirement of particular EMI applications without compromising the super hydrophobicity [40].

## **CHAPTER 3**

### **3. Synthesis and Characterization Techniques**

#### **3.1 Polymer Nanocomposite Synthesis Process**

In this dissertation, solvent evaporation technique is used to fabricate the composite film samples of polymethyl methacrylate (PMMA) loaded with CNFs into PYREX petri dishes.

##### **3.1.1 Solvent Evaporation:**

Solvent evaporation incorporates the solution/ dispersion to be evaporated in a controlled manner from the tiny holes created in the sheet which was used for uniform evaporation from composite dispersion with was deposited into the mould. Firstly, ready dispersion which was not much diluted not concentrated as well poured into the petri dish. Covered it tightly with Parafilm sheet and made holes on surface of parafilm for the evaporation of solvent from the composite solution. The substrate is first placed into a vacuum oven for 2 hours for uniform evaporation and after that when dispersion become smooth and stable, take it from vacuum oven and let it dry for 48 hrs. at room temperature to form a uniform and stable composite film. Usually, from more concentrated dispersion, evaporation rate is not uniform and composite materials become stressed, agglomerated in matrix material. Solvent evaporation depends on several material, dispersion and experimental process parameters which are manipulated to control the quality of the films. The density and molecular weight of polymer, evaporation rate of the solvent used for dissolving polymer, viscosity of the dispersion, non-uniformity of the surface, bubbles generation on the inner surface of parafilm which disturb the uniform evaporation, type of substrate used for deposition, temperature variation during evaporation, agglomeration of composite material due to lesser quantity than percolation threshold are the critical process parameters which are systematically optimized [41, 42].

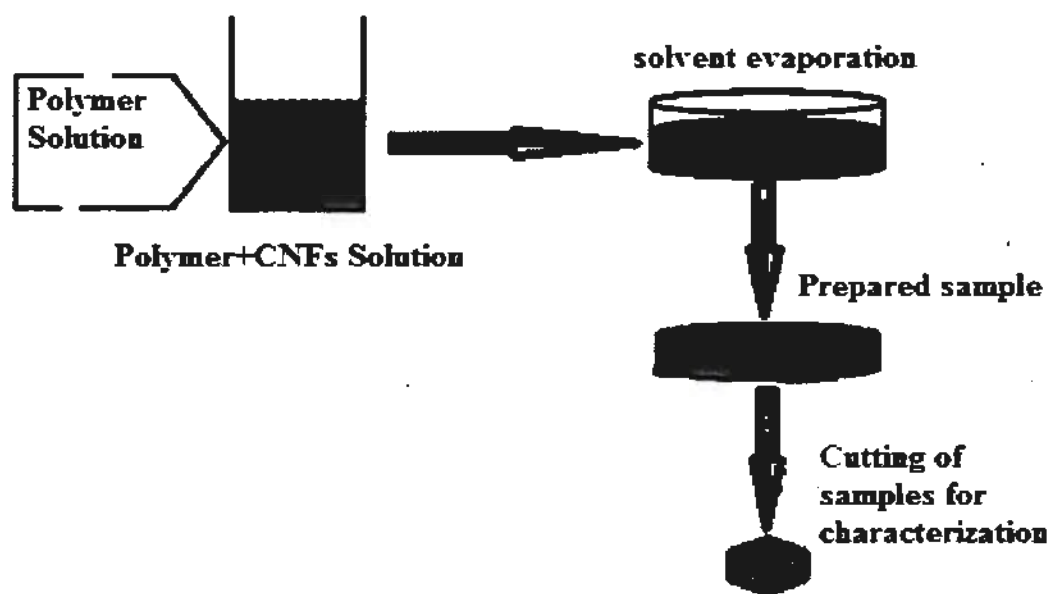


*Figure 3-1: Schematics of solvent evaporation*

## **3.2 Characterization Techniques:**

### **3.2.1 X-Ray Diffraction:**

X-ray diffraction technique is the most efficient method used to identify the crystallinity of the materials. Diffraction technique can characterize chemical compounds from their crystalline structure of the material. It indicates that the various chemical compounds or phases, having the identical composition can be determined[43, 44].

This technique is based on the Bragg's law. When the X-ray beams fall on the materials under test, which are diffracted through the crystallographic planes as illustrated in **Figure 3-2**. The 'beam 1' and 'beam 2' are incident in-phase on sample which are deflected and diffracted by two subsequent crystal planes. The deflected waves will never be in phase other than if Bragg's relationship is satisfied.

$$n\lambda=2d\sin\theta \quad (3.1)$$

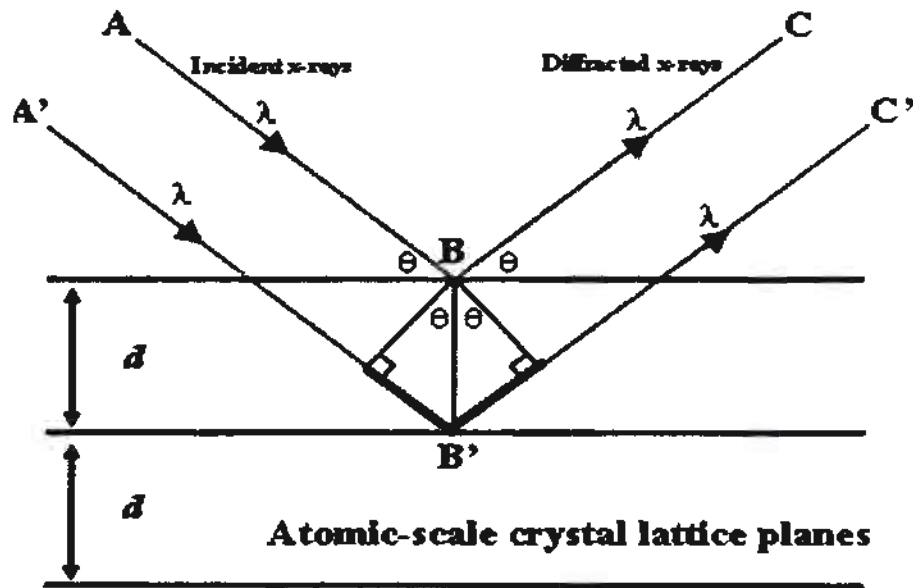


*Figure 3-2: Bragg's diffraction from the crystal planes*

Equation 3-1 is a fundamental law associated with diffraction known as Bragg's law relationship. Bragg's Law can be derived by finding the path difference between two beams in Figure 3-2. The path difference depends upon the incident angle  $\theta$  as well as the gap between parallel crystal planes ( $d$ ). For the two beams in-phase, the path difference ( $FG+GH=2d\sin\theta$ ) needs to equal to one or an integral multiple of X-ray wavelengths ( $n\lambda$ ) [45].

### 3.2.1.1 X-Ray Diffractometer:

X-ray diffractometer, the most commonly used method in material characterization, was initially applied for analyzing the actual crystallinity of powder samples; therefore, it is usually known as X-rays powder diffractometer [46]. An X-ray diffractometer comprises of a source of X-rays, the X-ray generator, a diffractometer assembly, and X-ray data collection and analysis system. The diffractometer assembly controls the alignment of the beam, as well as the position and orientation of both the specimen and the X-ray detector. X-ray diffraction requires monochromatic radiations, generated by excitation of K-radiations from a pure metal target and then filtering the beam by interposing a foil which strongly absorbs the  $\beta$ -component of the K-radiation without any appreciable reduction in the intensity of  $\alpha$ -component.



The scanning electron microscope (SEM) is capable of producing high resolution images of sample surface [48]. SEM indicates detailed 3D images in considerably higher magnification (up to 300000). The surface structure of nanocomposite, polymers, crack areas, nanoparticles, nanofibers and also nano coating can be imaged by means of SEM with excellent clarity [49].

In SEM, electrons are thermionically emitted from a tungsten or lanthanum hexaboride (LaB6) cathode filament towards an anode; alternatively electrons can be emitted via field emission (FE). The electron beam which typically has an energy range from a few keV to 50 keV, is focused by two successive condenser lenses into a beam of very fine spot size ( $\sim 5$  nm). The beam then passes through the objective lens, where pairs of scanning coils deflect the beam either linearly or in a raster fashion over a rectangular area of the sample surface. As the primary electrons strike the surface, they are inelastically scattered by atoms in the sample. Through these scattering events, the primary beam effectively spreads and fills a tear-drop-shaped volume extending about  $1\mu\text{m}$  to  $5\mu\text{m}$  into the surface. Interactions in this region lead to the subsequent emission of electrons which are then detected to produce an image. X-rays are produced when electrons interact with the sample atoms that are detected by an SEM equipped with energy dispersive X-ray spectroscopy. The three-dimensional resolution of the SEM is subject to the size of the electrons spot which in turn depends on the magnetic electron-optical system which produces the scanning beam. The resolution is also limited by the size of the interaction volume, or the extent of material which interacts with the electron beam. By comparing the distances between atoms, the spot size and the interaction volume are both very large, so the resolution of the SEM is not high enough to image down to the atomic scale. The advantages of SEM include the ability to image materials and the variety of analytical modes available for measuring the composition and nature of the specimen [49].

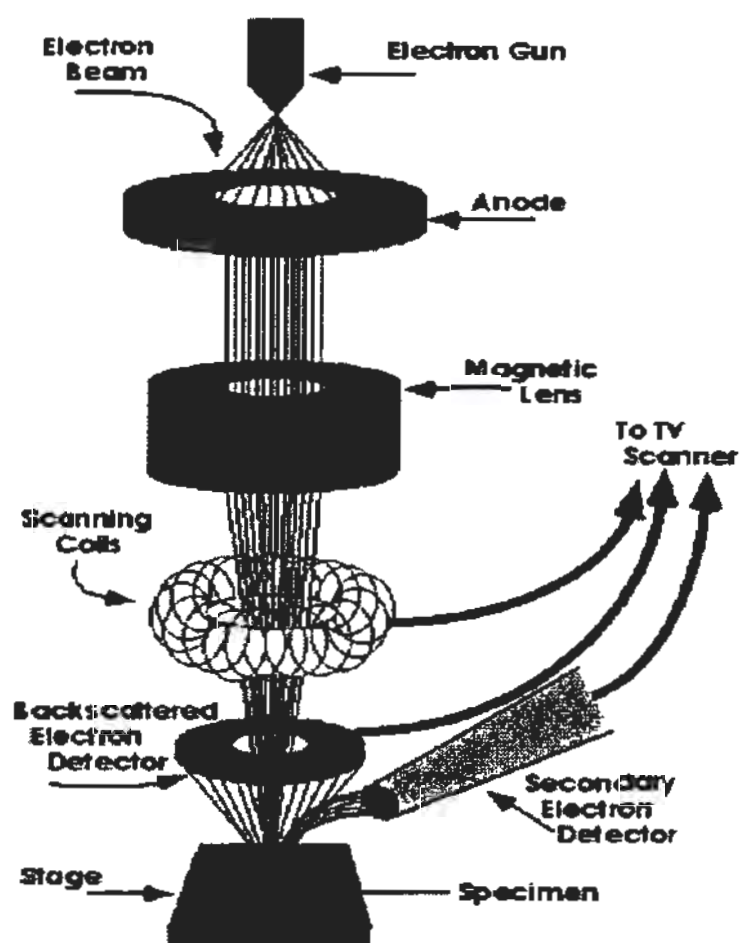


*Figure 3-5: Schematic diagram of SEM [49].*

### **3.2.3 Energy Dispersive X-ray Spectroscopy:**

Energy dispersive X-ray spectroscopy with SEM is the well-known and widely used for element analysis or chemical characterization. Along with low energy secondary electrons, backscattered electrons and X-rays are produced by the primary bombardment of electrons. The atomic number of element within the composite material is correlated with the intensity of backscattered electrons. Hence, by analyzing of characteristics X-rays emitted from the sample one can get more quantitative elemental information.

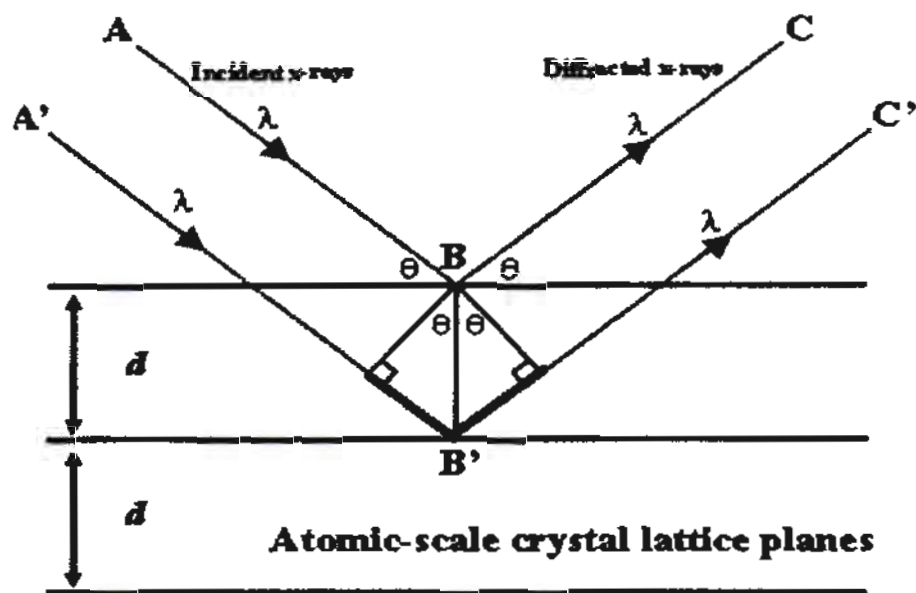
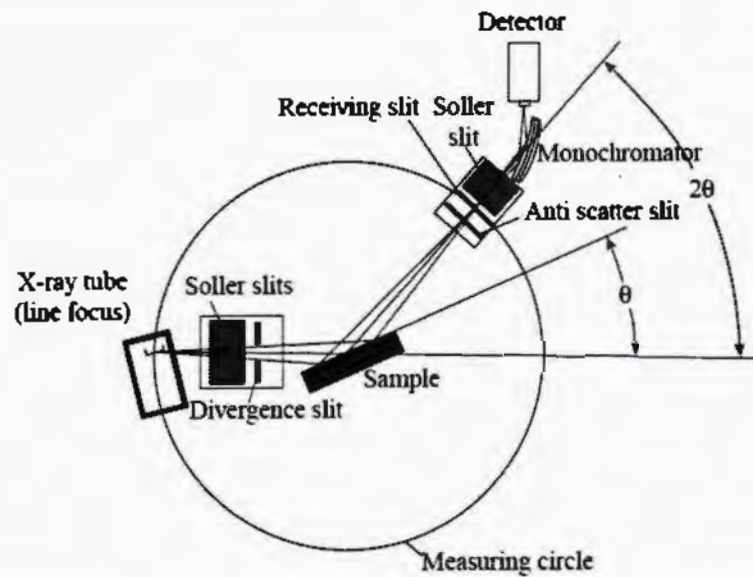


Figure 3-2: Bragg's diffraction from the crystal planes

Equation 3-1 is a fundamental law associated with diffraction known as Bragg's law relationship. Bragg's Law can be derived by finding the path difference between two beams in Figure 3-2. The path difference depends upon the incident angle  $\theta$  as well as the gap between parallel crystal planes ( $d$ ). For the two beams in-phase, the path difference ( $FG+GH=2d\sin\theta$ ) needs to equal to one or an integral multiple of X-ray wavelengths ( $n\lambda$ ) [45].

### 3.2.1.1 X-Ray Diffractometer:

X-ray diffractometer, the most commonly used method in material characterization, was initially applied for analyzing the actual crystallinity of powder samples; therefore, it is usually known as X-rays powder diffractometer [46]. An X-ray diffractometer comprises of a source of X-rays, the X-ray generator, a diffractometer assembly, and X-ray data collection and analysis system. The diffractometer assembly controls the alignment of the beam, as well as the position and orientation of both the specimen and the X-ray detector. X-ray diffraction requires monochromatic radiations, generated by excitation of K-radiations from a pure metal target and then filtering the beam by interposing a foil which strongly absorbs the  $\beta$ -component of the K-radiation without any appreciable reduction in the intensity of  $\alpha$ -component.



*Figure 3-3: Geometric arrangement of X-Ray Diffractometer [47].*

**3.2.2 Scanning Electron Microscopy:**

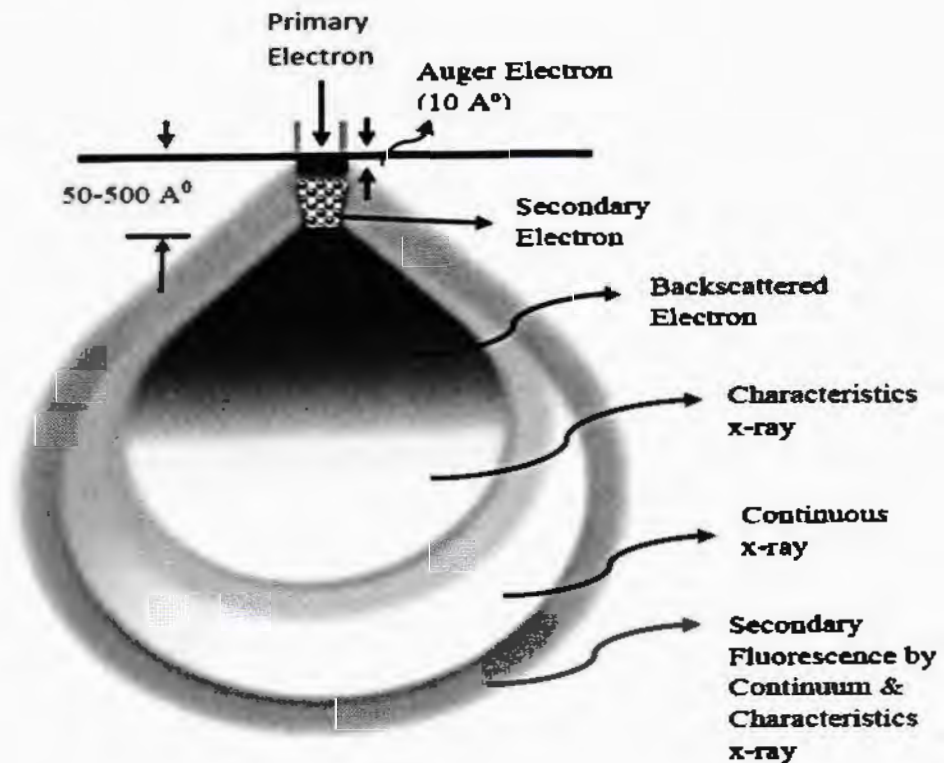


*Figure 3-4: Working principle of SEM.*

The scanning electron microscope (SEM) is capable of producing high resolution images of sample surface [48]. SEM indicates detailed 3D images in considerably higher magnification (up to 300000). The surface structure of nanocomposite, polymers, crack areas, nanoparticles, nanofibers and also nano coating can be imaged by means of SEM with excellent clarity [49].

In SEM, electrons are thermionically emitted from a tungsten or lanthanum hexaboride (LaB6) cathode filament towards an anode; alternatively electrons can be emitted via field emission (FE). The electron beam which typically has an energy range from a few keV to 50 keV, is focused by two successive condenser lenses into a beam of very fine spot size (~ 5 nm). The beam then passes through the objective lens, where pairs of scanning coils deflect the beam either linearly or in a raster fashion over a rectangular area of the sample surface. As the primary electrons strike the surface, they are inelastically scattered by atoms in the sample. Through these scattering events, the primary beam effectively spreads and fills a tear-drop-shaped volume extending about 1 $\mu$ m to 5 $\mu$ m into the surface. Interactions in this region lead to the subsequent emission of electrons which are then detected to produce an image. X-rays are produced when electrons interact with the sample atoms that are detected by an SEM equipped with energy dispersive X-ray spectroscopy. The three-dimensional resolution of the SEM is subject to the size of the electrons spot which in turn depends on the magnetic electron-optical system which produces the scanning beam. The resolution is also limited by the size of the interaction volume, or the extent of material which interacts with the electron beam. By comparing the distances between atoms, the spot size and the interaction volume are both very large, so the resolution of the SEM is not high enough to image down to the atomic scale. The advantages of SEM include the ability to image materials and the variety of analytical modes available for measuring the composition and nature of the specimen [49].

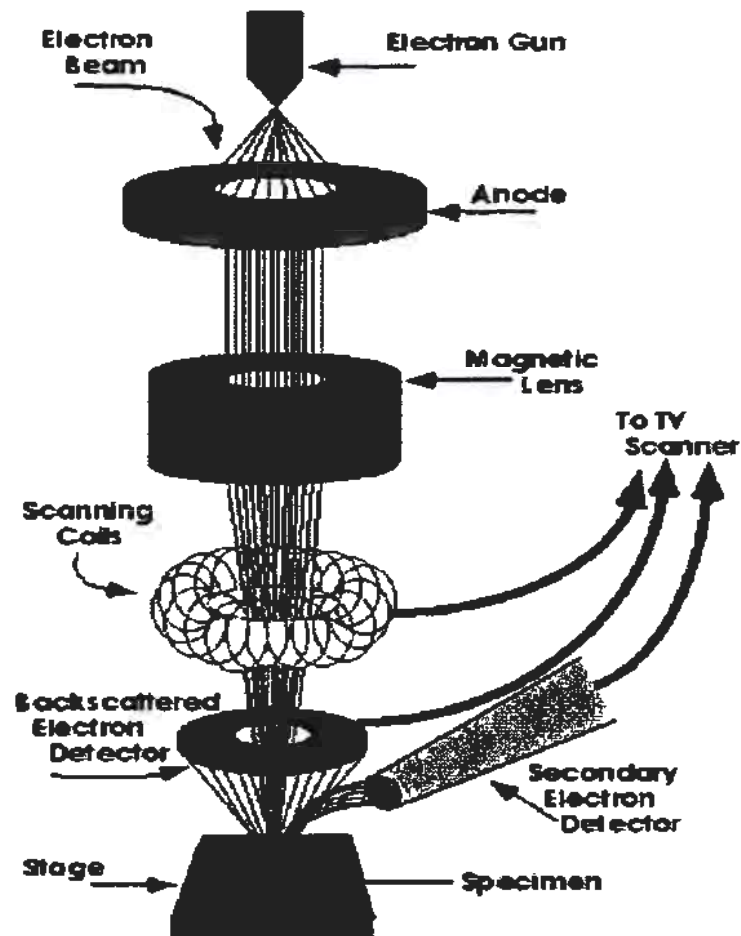


*Figure 3-5: Schematic diagram of SEM [49].*

### **3.2.3 Energy Dispersive X-ray Spectroscopy:**

Energy dispersive X-ray spectroscopy with SEM is the well-known and widely used for element analysis or chemical characterization. Along with low energy secondary electrons, backscattered electrons and X-rays are produced by the primary bombardment of electrons. The atomic number of element within the composite material is correlated with the intensity of backscattered electrons. Hence, by analyzing of characteristics X-rays emitted from the sample one can get more quantitative elemental information.



### 3.2.4 Fourier Transform Infrared Spectrometer:

Fourier Transform Infrared Spectrometry is one of the most popular spectroscopic techniques that have been successfully employed to study the organic and inorganic compounds in the materials. It is a nondestructive, rapid analysis method that needs small sample volumes and almost no interference of water fumes [50]. It is particular approach for identification of molecules, excites the vibrations of molecular bonds, for each vibrational frequencies every molecules possess distinctive fingerprint. When the photon interact with a molecules the Raman spectroscopy originate from inelastic scattering of UV, visible, or near IR light. The light which is scattered through a sample is detected into the individual wavelength by mean of spectrograph and then compiled in detector [51, 52].

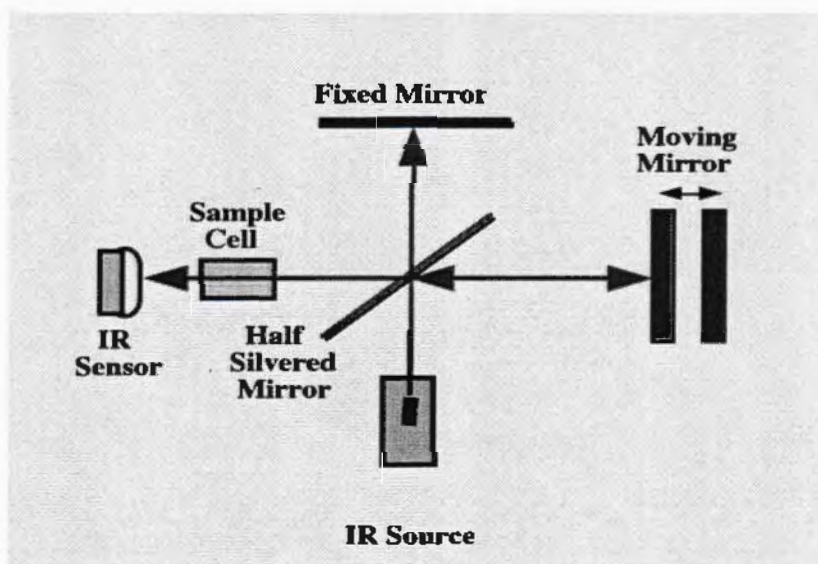


Figure 3-6: Schematics of FTIR Spectrometer [50]

The shown set-up works by shining the green IR radiation onto the sample through IR source, the sample absorbs a part of IR radiation and a part of it is transmitted. The resulting Infra-Red spectrum shows a characteristic region of the sample with absorption peaks consistent to the frequencies of vibration between the bonds of atoms making up the material. Each material has its own fingerprint region as material has different absorption at different frequencies of vibrations. Therefore, IR spectroscopy gives the good identification of all types of materials [52].

### 3.2.5 Four-point Probe Method (IV-Characterization)

The four-point probe method is the most common method of measuring resistivity. It is employed to measure surface resistance, in the Milli- or micro-ohm range, resistivity can be measured by two probe method, but the test contact resistance becomes a significant factor in two probe method that affect the measurement result. To eliminate the lead resistance or contact resistance, the four probe resistance measurement method is used [53]. Ohm's law is used to measure the resistance of any substance; it states the potential across a conductor is directly proportional to the current flowing through the conductor and inversely relate with the resistance of the conductor. Consequently, we can easily evaluate the resistance of conductor by using  $R=V/I$ : where V is applied voltage 'I' is current in a conductor and R is the resistance offered by conductor to the flowing current. Resistance of conductor also depends upon the temperature and geometry of the conductor. The geometry independent measure of resistance is given by resistivity ( $\rho$ ) and the reciprocal of resistivity is called conductivity ( $\sigma$ ) i.e.

$$\sigma=LA/R \quad (3.2)$$

Where L (m) is a certain length of the conductor A ( $m^2$ ) is an area of the conductor and R ( $\Omega$ ) is resistance across the conductor. The S.I unit of conductivity is S/cm [54]. The conductivity of the materials is measured by using the four-probe pointing method.

The four probe setup shown in figure 3-7 consists of four equal spaced tungsten metal tips with finite radius. To prevent the sample from damages during probing each tip is supported by springs and move up and down during measurement. A high impedance current pass through the 1 and 4 probes, a voltmeter is connected across the diagonally connected 2 and 3 probes to evaluate the resistivity of sample.

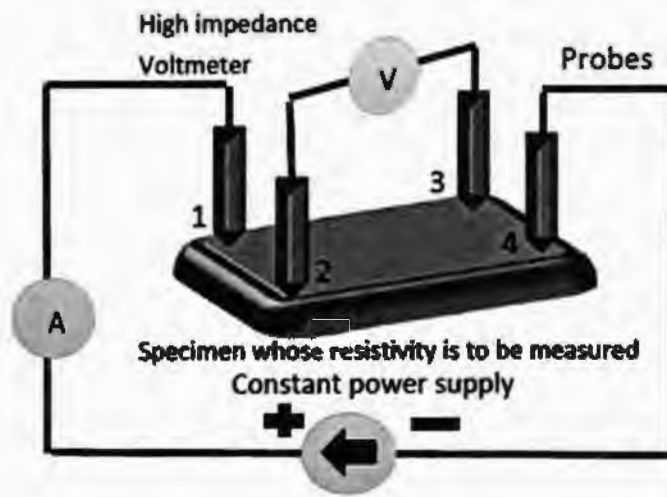


*Figure 3-7: Four probe method of measuring resistivity*

Normally probe spacing is nearly equal to 1mm. No current flows across 2 and 4 probe because of high input impedance voltmeter in the circuit. Therefore, undesired voltage drop ( $I R$  drop) at point 2 and 4 due to contact resistance between the probes and the sample is actually removed from the potential measurements. The current across the 1 and 3 probes, creates an electric field in the sample as shown in figure 3-8, the solid lines are drawn pointing the electric field lines and the equipotential lines are shown by broken lines [55].

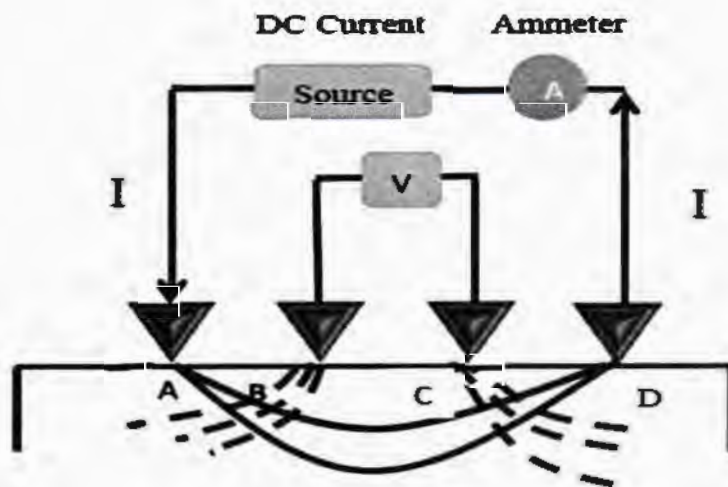


*Figure 3-8: Four probe method of measuring resistivity*

**3.2.6 Terahertz Time Domain Spectroscopy:**

Terahertz time domain spectroscopy (THz-TDS) has been widely employed for determining the variety of properties of materials, such as; THz transmission spectra, optical, dielectric properties, and thickness of materials [56]. THz-TDS is unique in its way of measuring the shielding effectiveness of thin film polymer-nanocomposites. In this technique, two electromagnetic pulses are measured: input pulse and transmitted pulse; the shape of input pulse changes due to its propagation through the sample under observation. Consequently, by fast Fourier transform (FFT) of the input and transmitted pulses in the time domain, the frequency dependent absorption in the sample can be calculated [56].

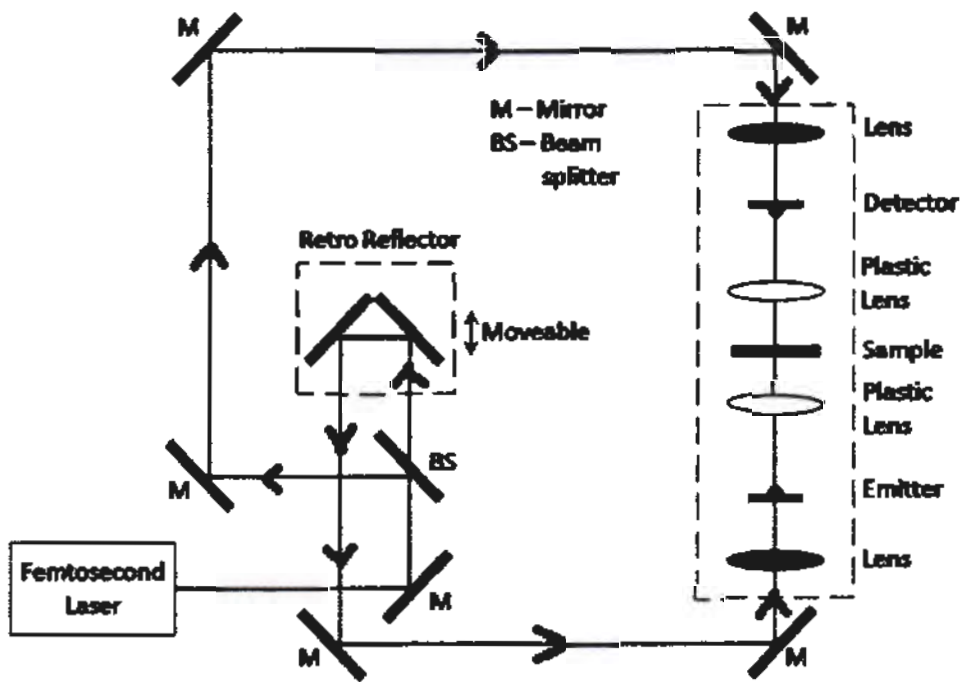


*Figure 3-9: Schematics of THz-TDS Technique*

In THz-TDS technique, pulsed laser having full width half maxima of 100 fs, and repetition rate of 80 MHz shine on the beam splitter and is divided into two beams: a pump and a probe beam. The THz pulses are generated and detected by two photoconductive antenna both acting as emitter as well as detector. The average power of both pump and probe beam is 50 mW and approximate distance between

emitter and detector is 30 cm. The voltage applied to THz emitter is synchronized with the transistor-transistor logic output of the lock-in amplifier. The output of THz detector (current in pA) is sensed by lock-in amplifier, after its per-amplification [57].

Schematic of the experimental setup used for THz-TDS (time domain spectroscopy) of nanocomposite films is presented in Figure. A 100 fs pulse at 780 nm is produced by Toptica's Femto Fiber Pro Laser System, which is subsequently split into two parts by a beam splitter. The maximum output power of the laser is ~100mW at ~80 MHz repetition rate, however, in this work ~45mW has been used. About 30 mW was focused onto the emitter photoconductive antenna (LT-GaAs, biased at 40V with modulation rate of 70 kHz), while the remaining ~15 mW was delayed by using a retro-reflector on a motorized linear stage and focused on the detector photoconductive antenna (LT-GaAs). Both photoconductive antenna have a built-in hemispherical silicon lens. The THz pulses as emitted from the emitter are focused on the sample using the hemispherical lens and a Teflon lens. The diverging pulses after passing through the samples were collected by a combination lens of Teflon lens and hemispherical lens, and it was ultimately focused on the detector. The current developed across the electrodes of the detector photoconductive antenna is measured by a lock-in amplifier (SRS model SR830) [57]. The current as a function of delay introduced by the retro-reflector is proportional to the electric field of the THz pulse. To reduce the absorption due to the moisture, the setup was purged to a humidity level of <10% using dry nitrogen (N<sub>2</sub>) gas. The THz pulse with and without sample is collected and converted into spectra by fast Fourier transform (Cooley-Tukey algorithm) using LabView.

## **CHAPTER 4**

### **4 Materials and Methodology:**

#### **4.1 Materials:**

The materials used in this research work were selected on the basis of their properties, commercial availability and cost effectiveness. The basic polymer used in this project work as a matrix are PMMA (polymethyl methacrylate) ( $M_w=99600$  by GPC) in crystalline form and was purchased from Sigma Aldrich Co. UK. PMMA has a good interfacial adhesion and its particles disperse stably which ultimately lead to reduction of surface energy of composite film. The CNFs (GNF-100, Carbon Nano-material Technology Co., Ltd. Korea) used as filler to give high electrical conductivity to the composite, while maintaining a relatively low cost and availability in large quantity. All of these materials were used as received.

#### **Solvents:**

The following solvents were used in this experimental work for the better dispersion of solid materials; Acetone (99.5%,  $M=58.08\text{g/mol}$ , Panreac Quimica SA), Toluene (99.5%,  $M=92.14\text{ g/mol}$  Sigma-Aldrich Co, UK), whereas ethanol was used for rinsing purpose.

#### **4.2 Method:**

This research work primarily utilized solution mixing method to make a uniform and stable dispersion of polymers and CNFs blend that is being used to develop a composite film into a PYREX petri dish used as mould by solvent evaporation.

##### **4.2.1 Weight percentage:**

In this experimental work, all materials were measured in weight percentage. This means that the concentration of polymers in solvents as well as concentration of CNFs was determined by calculating the weight percentage of the materials.



$$\text{desired quantity of material in gram} = \text{wt}\% \frac{(a)(b)}{100}$$

Here “b” is total solution “a” is a dry mass of materials in weight percentage of total solution. Similarly, CNFs loading concentration was obtained relative to the dry mass of polymers. Materials used in this research work were weighed using precision balance (Mether AE163).

## 4.2.2 Sample preparation:

S. No	PMMA (grams)	Acetone (ml)	Stirring Time	T. Sol. ml	CNFs (wt %)	Acetone (ml)	Probe Sonication time	Total Sol.	Magnetic Stirring time	Drying in Oven	Drying at Room temp.
1	2g	10ml	24 hrs	23.5 ml	-	-	10 min.	17ml	45 min.	2 hrs	48 hrs
2	2g	10ml	24 hrs	23.5 ml	0.05g (2.5wt %)	5ml	10 min.	17ml	45 min.	2 hrs	48 hrs
3	2g	10ml	24 hrs	23.5 ml	0.1g (5wt %)	5ml	10 min.	17ml	45 min.	2 hrs	48 hrs
4	2g	10ml	24 hrs	23.5 ml	0.15g (7.5wt %)	5ml	10 min.	17ml	45 min.	2 hrs	48 hrs
5	2g	10ml	24 hrs	23.5 ml	0.20g (10wt %)	5ml	10 min.	17ml	45 min.	2 hrs	48 hrs
6	2g	10ml	24 hrs	23.5 ml	0.25g (12.5wt %)	5ml	10 min.	17ml	45 min.	2 hrs	48 hrs

Table 4-1: Solution compositions employed for synthesis of polymer-CNF composites

To prepare composite thin film of polymers-CNFs blends i.e. PMMA, firstly reference/ control sample was developed consisting of only polymer. PMMA which was dissolved in acetone. The 20wt% of PMMA dispersion was developed by dissolving 2g polymer in 10ml of acetone by stirring constantly on hot plate (Heidoph MR2002) having magnetic stirrer at 60°C/ 250 rpm speed for 6 hrs. When the polymer was completely dissolved into solvent, then 12ml solution of polymer was ready for the fabrication of samples by solvent evaporation. Then this solution was deposited into the PYREX petri dishes of diameter 2 inches using as substrate. These PYREX petri dishes were then wrapped by the parafilm and then made small holes on the whole surface of it for the uniform evaporation of Solvent. After the deposition and wrapping, film was heat treated in the Oven (Model # MEMMERT VO-200 German) to make it lasting on a substrate properly and to maintain the evaporation rate of solvent. Similarly, loaded samples were developed by making a solution of PMMA of 12 ml by following the procedure as mentioned above loaded with various loadings of CNFs wt% w.r.t the solid mass of polymers as mention in above Table 4-1. Firstly, CNFs were ultrasonically dispersed in 5 ml Acetone using a Probe Sonicator for 10 minutes with a pulse of 1 minute. The stable dispersions of CNFs were obtained in acetone. The suspensions of CNFs were then mixed into the as prepared polymer solution of 12 ml. The mixture was again ultra-sonicated for 10 minutes with a pulse of 1 minute in a probe sonicator to obtain a uniform dispersion of CNFs in PMMA solution. And then these stable dispersions were used to fabricate nanocomposite films on a substrate by the same procedure as were adopted to prepare of the reference sample.

4.2.3 Flowchart of Experimental Work:

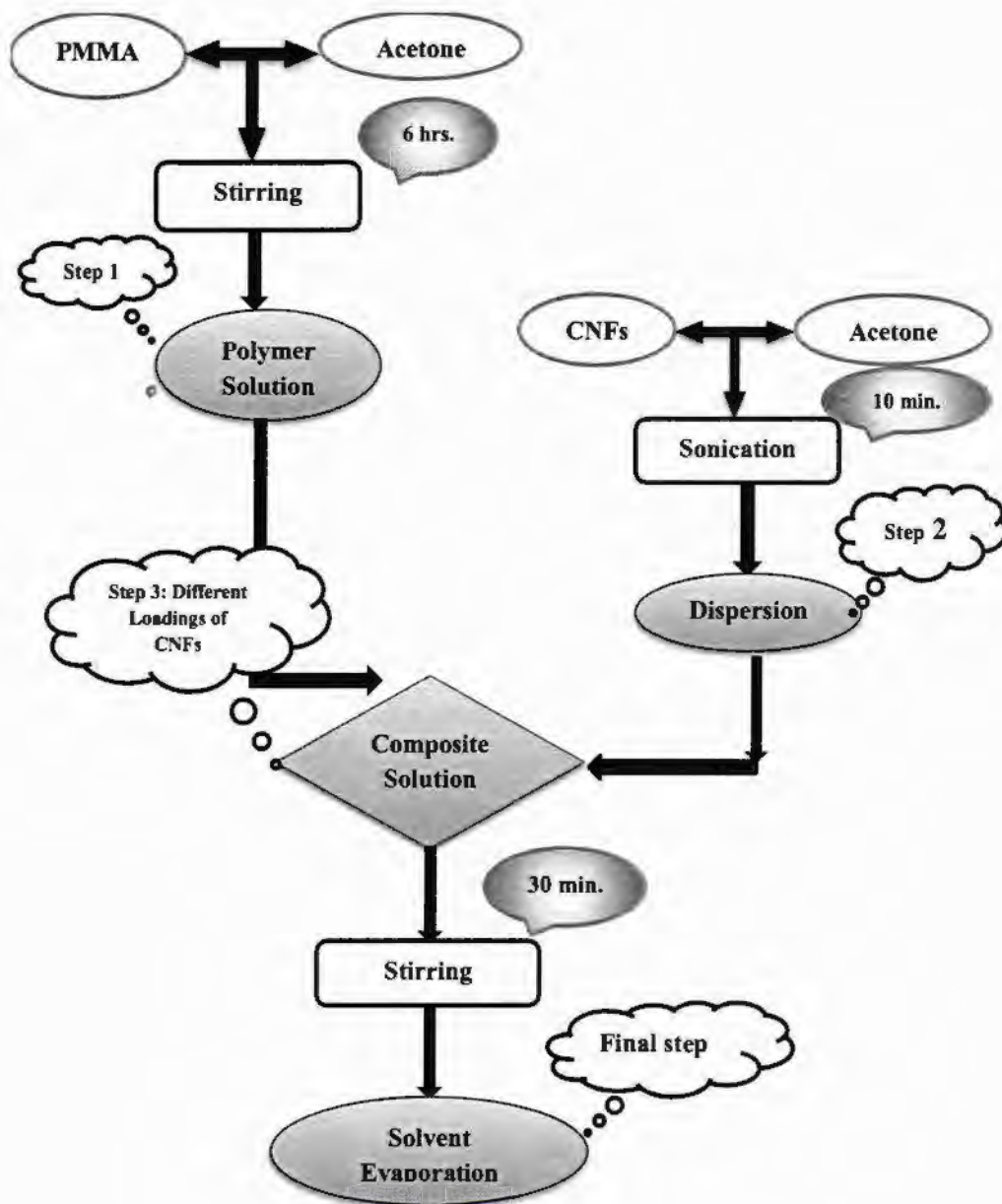


Figure 4-2: Flowchart

## **CHAPTER 5**

### **5 Result & discussion:**

#### **5.1 Optimization of Process Parameters:**

A number of technical challenges came on a way while making the polymer nanocomposite films on the glass substrate by solvent evaporation as regards to the consistency of the solution and preparation of nanocomposite film that required optimization by adjusting the parameters of solution and solvent evaporation rate.

##### **5.1.1 Hydrophobicity**

One of the leading issue while making composite films by solvent evaporation was hydrophobicity in the samples. This happened because of low concentration of CNFs as compared to the polymer, i.e. PMMA. This issue was resolved by readjustment of wt. % of CNFs compared to the Polymer solution and by increasing the ultrasonication time.

##### **5.1.2 Evaporation time**

The other problem encountered in the way while solvent evaporation, that solvent was not completely evaporated we peeled off samples from the petri dishes. It caused stresses in the composite film which is not completely dried. This issue was resolved by increasing the evaporation time to completely dried the samples.

##### **5.1.3 Center to Edge Thickness Variation**

While pouring the solution into Petri dishes, after evaporation, the thickness of film was found to vary from center to edges.

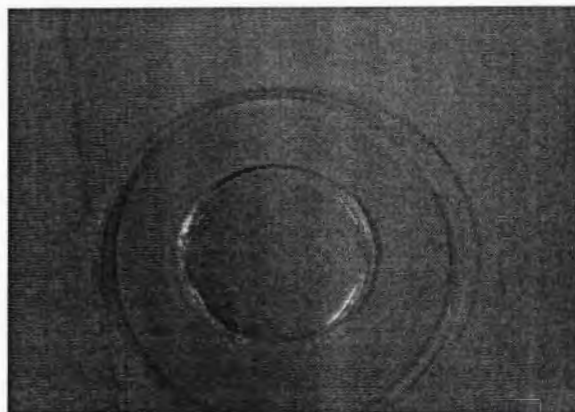


*Figure 5-1: Thickness Variation.*

This was believed to be due to the improperly pouring polymer solution into petri dishes and was needed to adjust the concentration of polymer solution to make sure that it was evenly poured film into the whole substrate, resulting in the uniform films.

#### **5.1.4 Temperature Variation**

Another major issue during evaporation of solvent was the variation in the temperature as it varies from day to night which affects the uniform evaporation of solvent. Due to this temp. variation, bubbles generate at the inner surface of Parafilm which reduces the evaporation rate. This issue was resolved by first heat treated the samples in the Oven at temperature  $35^{\circ}\text{C}$  for 2 hrs. and then samples dried at room temperature for 2 days.

#### **5.1.5 Film Stiction**

The adhesion of film was another problem was faced after solvent evaporation from the polymer solution into the glass petri dishes.

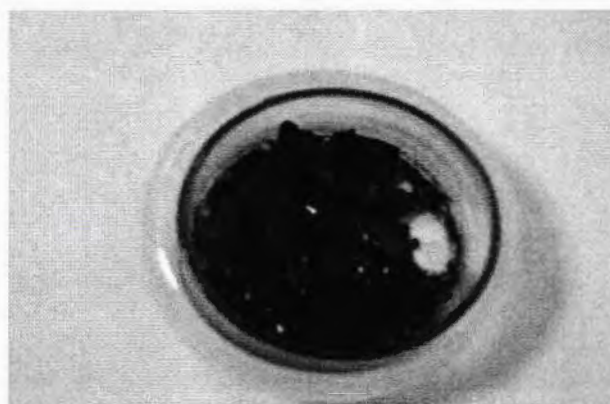
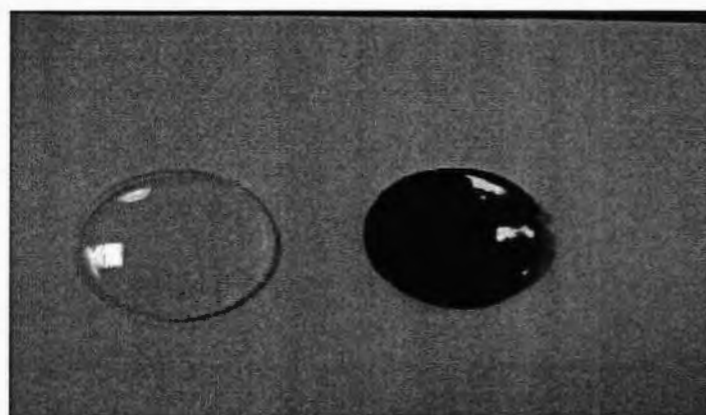


*Figure 5-2: Adhesion issue.*

This happened because of the solvent (Toluene) we used, for the stable dispersion of CNFs, is enough to give strong adhesion with glass, so that one could not peel off that composite film from glass Petri dish and as the sample was heat treated after solvent evaporation bubbles appear in the whole film and melted like, be apt to film not peel off from the substrate. This problem was resolved by using Acetone for the dispersion of CNFs as well instead of Toluene.

### 5.1.6 Optimized samples

Finally the optimized films were developed, confronting with all issues and parameters, by adjusting the solution viscosity and quantity, solvent evaporation rate, and dispersion time etc.



(a) Control

(b) Loaded

*Figure 5-3: Optimized Samples*



## 5.2 Results

### 5.2.1 XRD Analysis

XRD analysis was used to study the crystal structure and phase behavior of PMMA solution in presence of CNFs. The D8 Discover HR-XRD (BUKER axs, Germany) using  $\text{CuK}\alpha$  radiation with a wavelength  $1.54\text{\AA}$ , were used at DMME in PIEAS for characterization of polymer/CNFs composite films.

The sample was placed at sample holder in diffractometer and was characterized by the method as describe in 3.2.1.1 section. The measurements were taken between  $2\theta$  values of  $10 - 90^\circ$  with a scan rate of 2 degree per min and step size  $0.02^\circ$ .

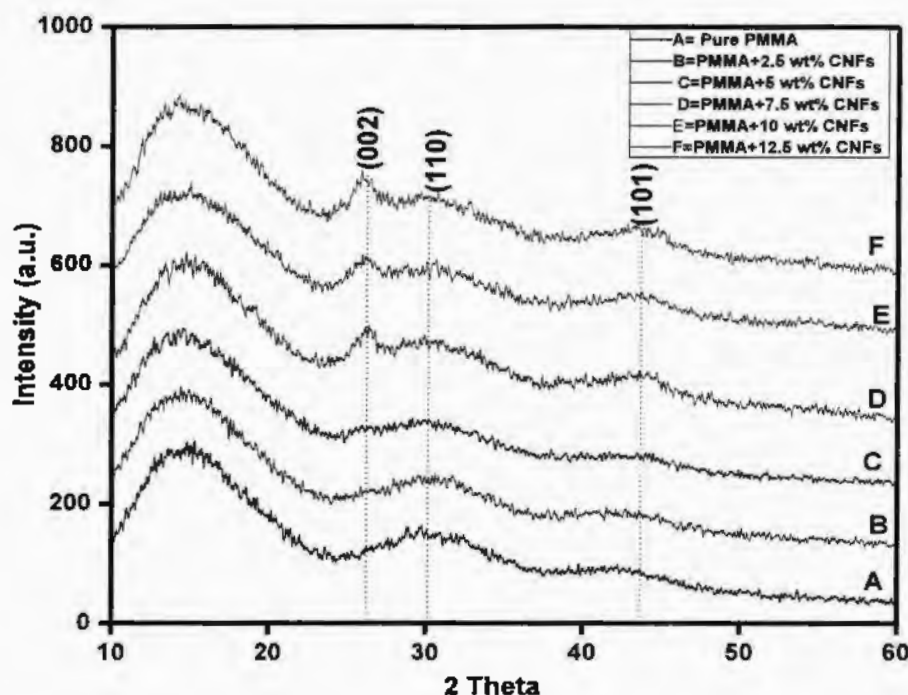


**Figure 5-4:** XRD patterns of PMMA composite film with different loadings of CNFs (A) reference sample (B) 2.5wt% loading of CNFs (C) 5wt% loading of CNFs (D) 7.5wt% loading of CNFs (E) 10wt% loading of CNFs (F) 12.5wt% loading of CNFs

Figure shows the XRD pattern for the pure PMMA as reference sample and PMMA with different loading of CNFs i.e. from 2.5wt% to 12.5wt%, respectively. The characteristic peak of PMMA was observed at  $2\theta$  angle of value

14.79° corresponding to the lattice plane (100). From above graphs, it is clear that there are two dominant diffraction peaks of PMMA+CNFs at  $2\theta=26.6.0^\circ$  and  $2\theta=43.6^\circ$  with planes (002) and (101) respectively confirms the hexagonal graphite structures of planes. Whereas, given information confirms the amorphous nature of different loadings of CNFs/PMMA nanocomposite film with broad diffraction peaks at  $2\theta =17^\circ$  and  $2\theta =32^\circ$  corresponding to the PMMA matrix which determined the overlapped peaks of PMMA and CNFs [58, 59]. The distinctive peak of CNFs was observed at  $2\theta = 26.31^\circ$  corresponding to the lattice plane (002) that shows the structure of CNFs has not changed during chemical modification. The absence of CNFs diffraction peaks in the XRD pattern with loading of 2.5 wt% in the nanocomposite film is due to the homogeneous dispersion and very low weight percentage of CNFs in the PMMA as the percolation threshold in our case was 5wt% of CNFs .

### **5.2.2 FTIR Analysis**

FTIR analysis was used to identify chemical bonds in a molecule by producing an infrared absorption spectrum i.e., of PMMA solution in presence of CNFs. The Nicole-6700 (Thermo Corporation) using 6 resolution rate with a spectrum range from 400-4000, was used at PIEAS in nanotechnology lab for characterization of polymer/CNFs composite film.

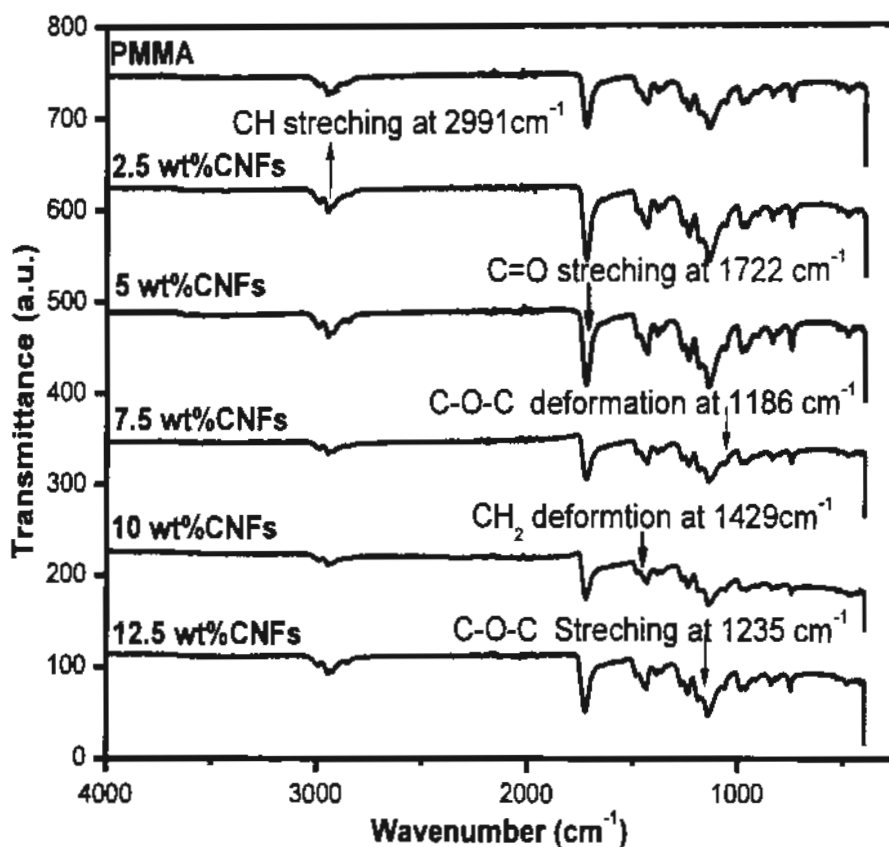


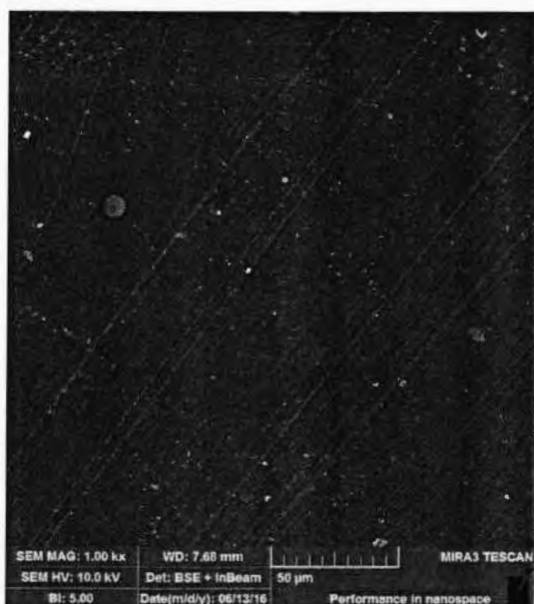
Figure 5-5: FTIR Spectra of Samples

So as to study and understand the intermolecular interactions between the polymer and CNFs, FTIR analysis was performed. There were no major differences in the spectra of PMMA and PMMA-CNFs above  $1,800\text{ cm}^{-1}$ . In the region from  $1800\text{ cm}^{-1}$  to  $900\text{ cm}^{-1}$ , there are remarkable changes, and the PMMA peaks were based on earlier reported work. In PMMA, the C=O ester appears at  $1710\text{ cm}^{-1}$  with a slight peak at  $1722\text{ cm}^{-1}$ . Though, this small shoulder shifted to  $1727\text{ cm}^{-1}$  for PMMA-CNFs, clearly signifying the existence of chemical interfaces between the C=O group and CNFs. Furthermore, the C=O band for PMMA-CNFs is broader than the corresponding band for electrospun PMMA, which proposes two different chemical surroundings in the C=O structure. At  $1429\text{ cm}^{-1}$ , comparable increase in peak width was observed in the band of PMMA, which agrees to the skeletal  $\text{CH}_2$  deformation. The analogous band for PMMA-CNFs was moved towards higher wavenumbers and broadened to a  $1432\text{ cm}^{-1}$ – $1450\text{ cm}^{-1}$  range. C–O in the ester group corresponds to the bands at  $1233\text{ cm}^{-1}$  and  $1265\text{ cm}^{-1}$  for PMMA, did not suffer significant modifications of their width, but were shifted to  $1238\text{ cm}^{-1}$  and  $1268\text{ cm}^{-1}$  for PMMA-CNFs. Finally, the bands that correspond to C–O–C of the methoxy group and

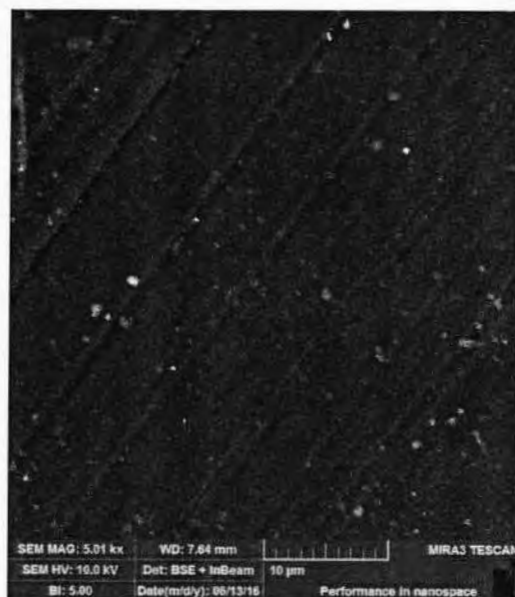
skeletal C–C for PMMA appear at  $1137\text{ cm}^{-1}$  and  $1186\text{ cm}^{-1}$ . For PMMA-CNFs, bands were highly affected in their shape and moved towards  $1146\text{ cm}^{-1}$  and  $1191\text{ cm}^{-1}$ . In PMMA/CNFs composite spectra, two bands at  $2,997\text{ cm}^{-1}$  and  $2,952\text{ cm}^{-1}$  can be assigned to the C–H bond stretching vibrations of the –CH<sub>3</sub> and –CH<sub>2</sub>– groups, respectively [60].

### 5.2.3 FESEM Analysis

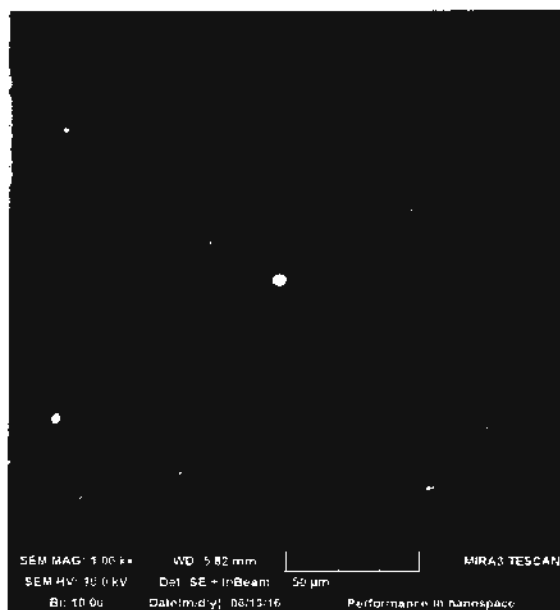
Field emission scanning electron microscopy (FESEM, MIRA3 Tescan) was used at Department of Materials Science and Engineering in IST, to observe the surface morphology of PMMA film and the dispersion of CNFs of different loading in PMMA solution at an accelerating voltage of 1.0 KV and 5.0 KV. The few sample surfaces were coated with a thin layer of carbon by means of sputter coater before SEM analysis to make them conducting and avoid samples surface from charging.



a) Surface View of Pure PMMA



b) Pure PMMA



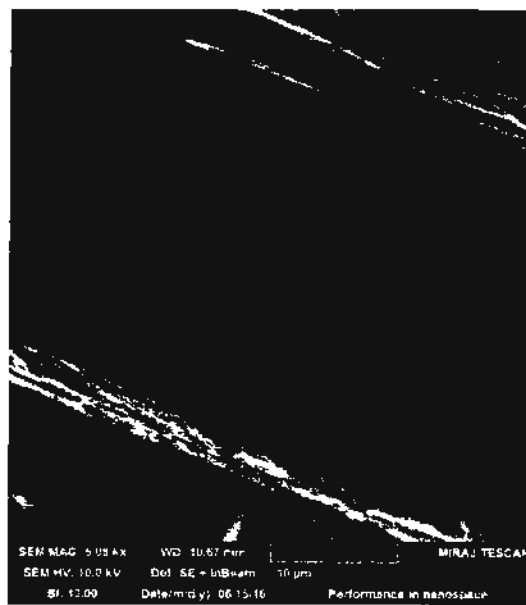
c) PMMA+5wt% CNFs



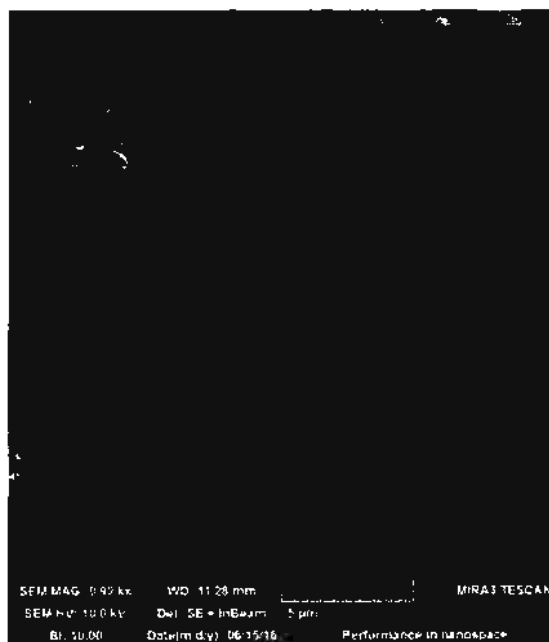
d) PMMA+5wt% CNFs



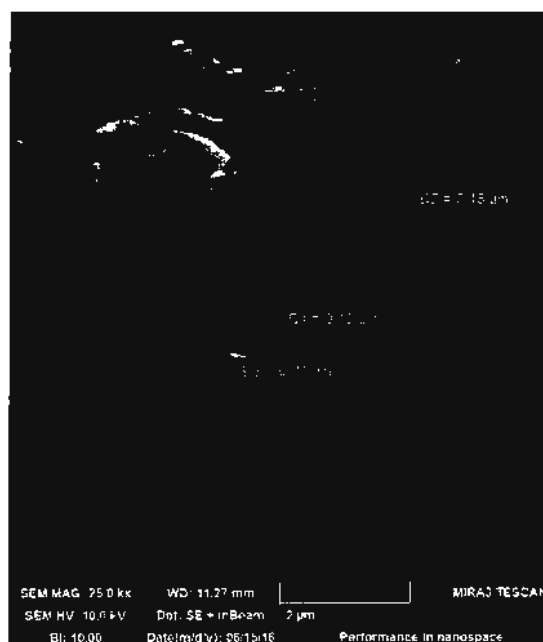
e) Crosssectional view of Pure PMMA



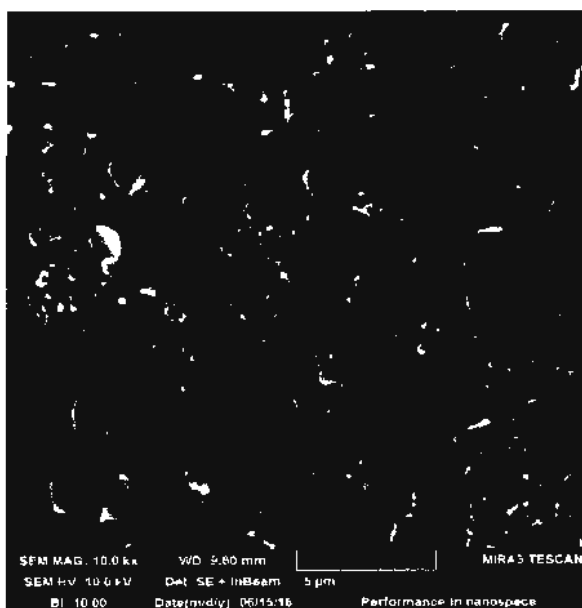
f) PMMA with 2.5wt% CNFs



g) PMMA with 10wt% CNFs



h) PMMA with 10wt% CNFs



i) PMMA with 12.5wt% CNFs



j) PMMA with 12.5wt% CNFs

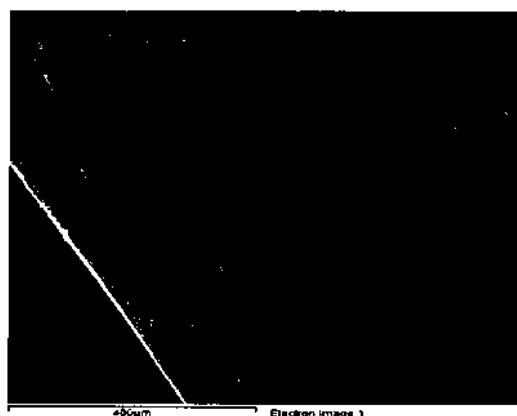
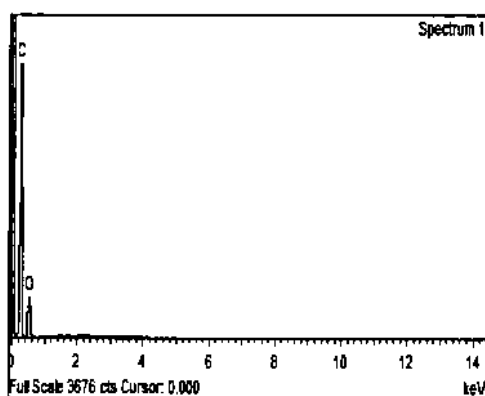
Figures 5-6: (a-j) show the SEM micrographs and top view of surface morphology of pure polymer PMMA and PMMA composite film with different loading of CNFs from 2.5wt% to 12.5wt% respectively at 50 $\mu$ m and 10 $\mu$ m magnification

Scanning electron microscopy was used to observe the dispersion and distribution of nanofibers within the polymer PMMA used as a matrix for these composite films. Topical view of micrographs gives us not enough information even at higher magnification. So we move on crosssectional micrographs which give us detailed information about the behavior of CNFs inside the polymer matrix. Here some figures show the fracture surface of the composite films which is due to hardness of the composite films. CNFs are well dispersed as also clearly seen in all the PMMA/CNFs composite films. Surface uniformity is also an enormous factor while making these samples by solvents evaporation.

Figure (e-j), are the representative micrographs of cross-sectional fracture view from where dispersion of CNFs is clearly observed. All specimens are mounted such that the plane viewed under the microscope was cross-sectional cut perpendicular to the extrusion direction. In figure e, cross-sectional view of pure polymer shows that polymer itself contains carbon chain. In the figure (g-j) pulled-out CNFs and holes are observed. These holes might have created when the CNFs were being pulled-out [61, 62]. And diameter of CNFs is measured in these micrographs ranging between  $0.15\mu\text{m}$ -  $0.29\mu\text{m}$ .

#### 5.2.4 EDX Analysis

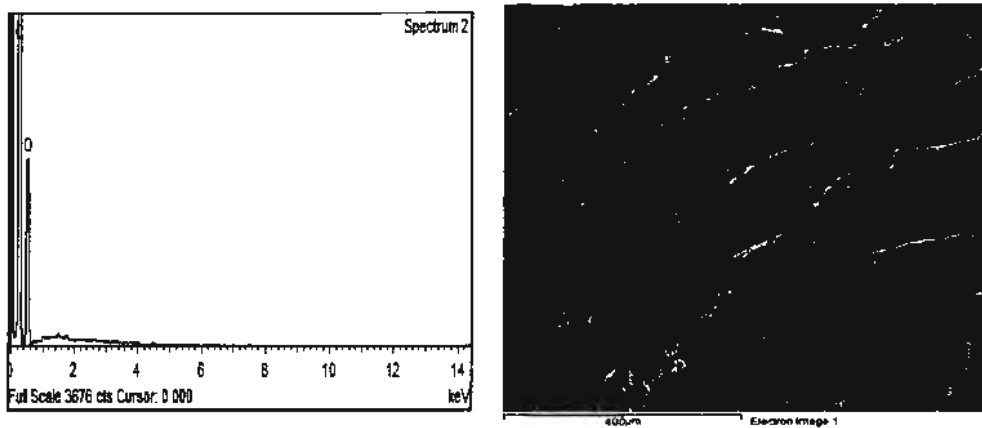
Energy dispersive x-ray spectroscopy mounted in Field emission scanning electron microscopy (FESEM, MIRA3 Tescan) was used to study the quantitative amount and distribution in composite films.





Element	Weight%	Atomic%
C K	67.02	73.02
O K	32.98	26.98
Totals	100.00	

**Figure 5-7:** EDX Characteristics of CNFs Dispersed in PMMA Polymer Matrix.



Element	Weight%	Atomic%
C K	69.04	74.82
O K	30.96	25.18
Totals	100.00	

**Figure 5-8:** EDX Characteristics of CNFs Dispersed in PMMA Polymer Matrix

By using EDX, the presence and distribution of chemical elements on the fractured samples could be determined, the software maps the elements found on the SEM image by X-ray analysis. One can make estimation of the quantity of the elements in terms of atomic and weight percentages.

The EDX quantitative analysis showing that these composite films contain Carbon and Oxygen. Here EDX data also shown that the carbon is prevailing in the composition of PMMA+CNFs nanocomposite films with 69% by weight. The dominance of carbon confirms the amount of Polymer which itself contains long

chains of carbon and experimentally employed CNFs during the synthesis of composite film.

### 5.2.5 Four Point Probing Method

Four point probing method in the Model4200-SCS's Keithley Interactive Test Environment (KITE) was used to measure Electrical Conductivity in the Advanced Characterization Lab at NILOP. The  $1\text{mm}^2$  samples were used to characterize by applying silver paste contacts to develop the contact between samples and probes. -25 $\mu\text{A}$  to 25 $\mu\text{A}$  current is supplied to the two opposite sides connected probe and voltage is being measured from other two probs

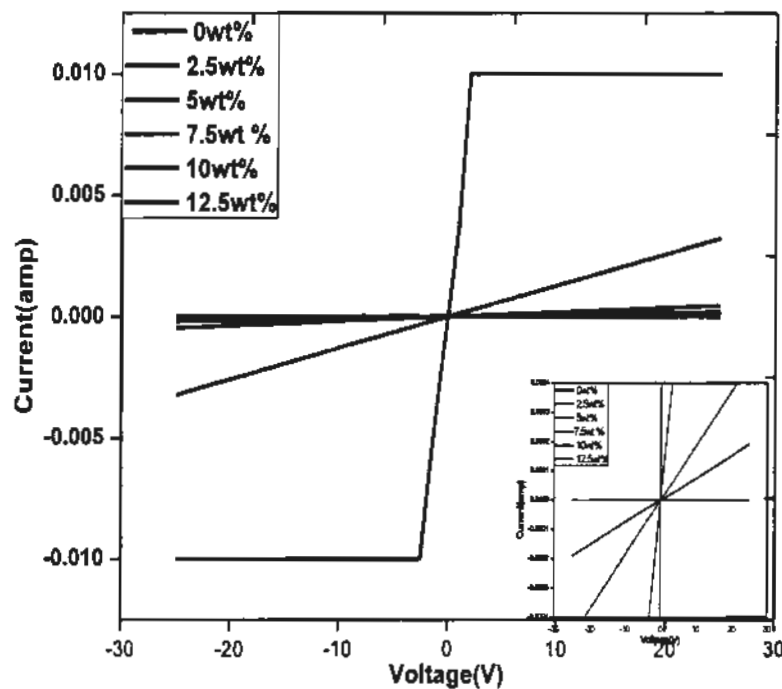


*Figure 5-9: Electrical Characteristics of CNFs Dispersed in PMMA Polymer Matrix*

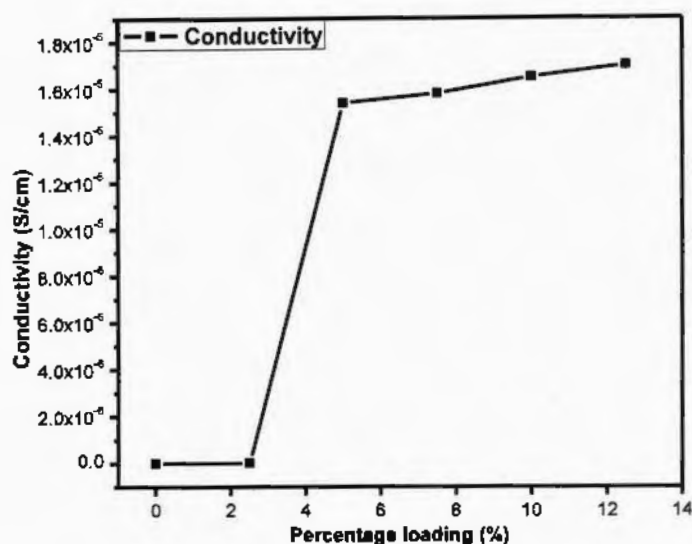


**Figure 5-9:** Electrical Characteristics of CNFs Dispersed in PMMA Polymer Matrix

It is known that the polymers without doping behave like an insulator. We here determine the electrical properties of polymer nanocomposite films. Near the percolation threshold, by adding the CNFs content in the polymer base matrix, the properties of polymer composite are changed dramatically from insulating material to the conducting material. In this case, Percolation Threshold was 5 wt% to the solid mass of polymer. At the low CNFs concentration in a polymer matrix, the composite film behaves mostly like an insulator i.e., at 2.5wt% of CNFs. A conductivity enhancement of the order of 6 has been observed with conductivity value from  $0.79 \times 10^{-10}$  S/cm to  $0.170 \times 10^{-4}$  S/cm in the sample having 12.50wt% of CNFs. By increasing the CNFs concentration in polymer matrix the possibility of electron tunneling between neighboring cluster increases as well as the conduction path develops through the composite film, which leads to a decrease of resistivity in film. At the higher loading of CNFs the maximum resistivity is decreased. And so, it reveals that the electrical properties change drastically over a small composition range [58]. In our case the conductivity is increase of several orders of a magnitude with increasing percentage loading from 5wt%-12.5wt% in polymer matrix. At its maximum loadings of CNFs in the polymer matrix i.e., 10 wt% and 12.5 wt%, *saturation regions* in both cases gives us very useful information that electronic circuits may breakdown after applying higher voltage to the circuit. Straight line in

the conductivity graph shows saturation region that should not go further than that limit.

### 5.2.6 THz-TDS Analysis

Terahertz Time domain spectroscopy was used at Tera-Hertz Spectroscopy in NILOP to analyze the shielding effectiveness due to attenuation losses of EM radiation, transmitted through the sample in the 0.2 THz-1.2 THz frequency range. The erbium doped fiber laser with pulse width of 100 fs and 80 MHz repetition rate used as a pulse source in THz-TDS.

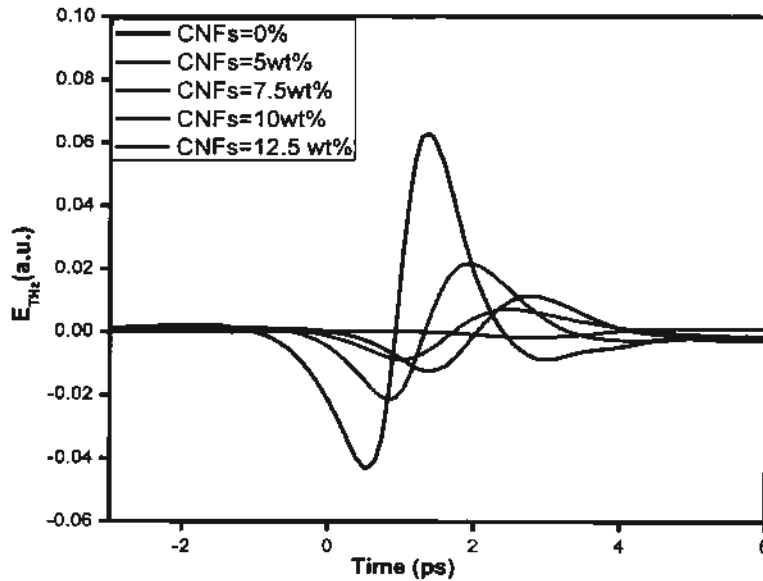


*Figure 5-11: THz electric field amplitude in time domain of reference sample and polymer nanocomposite with different loading of CNFs.*

Figure 5-11 shows the THz electric field amplitude in the time domain of the reference sample which is pure polymer PMMA and the composite film of polymer blend as a matrix with the different weight percentage loading of CNFs. The results show that the peak of electric field amplitude is decreasing with increasing percentage loading of CNFs in polymer matrix from 0wt%-12.5wt%, this is due to increase in conductivity value from  $0.79 \times 10^{-10}$  S/cm to  $0.170 \times 10^{-4}$  S/cm with loading [61, 62]. It is concluded that attenuation of electric field is increased with increasing the CNFs

loading, which agrees well with previous observations. The peak shifting from reference sample to the loaded samples of polymer nanocomposite shows the thickness variations between loaded and unloaded samples as well as slight change in refractive index.

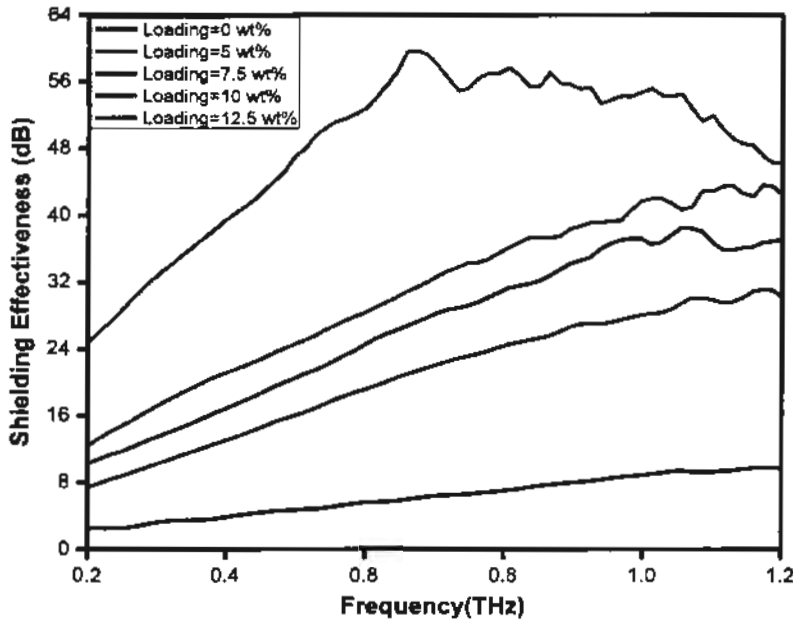


*Figure 5-12: Shielding Effectiveness in THz frequency range 0.2-1.2 THz*

In figure 5-12 the shielding effectiveness of the reference sample and loaded samples with polymer nanocomposite were calculated from the time-domain measured data in 0.2 to 1.2 THz frequency range. The shielding effectiveness is calculated as  $SE=20 \log E_r/E_s$ , where  $E_r$  is taken as reference sample and  $E_s$  is the transmitted electric field through the sample [63]. In the frequency domain the shielding effectiveness or rate of absorption is increased with increasing frequency and loading parentage of CNFs, due to skin effect i.e. at high frequencies the EM radiation penetrates to the surface of conducting material, so the thin film of polymer nanocomposite with increasing conductivity shows the good SE at high frequency.

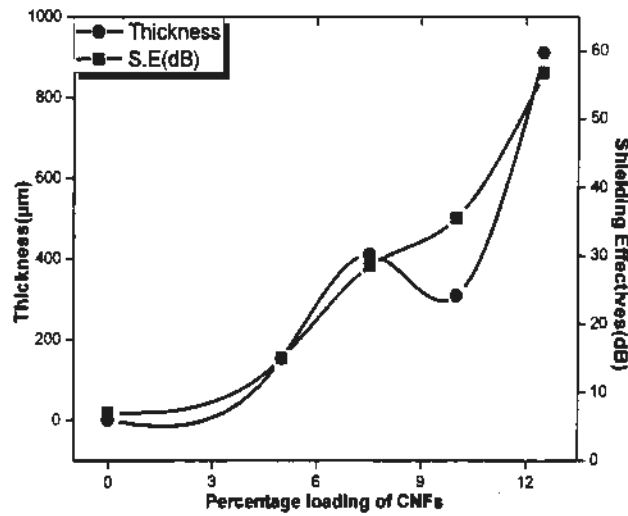


Figure 5-13: Increase of Shielding effectiveness with variation of Thickness

Figure 5-13 shows how shielding effectiveness correlates with Thickness. Shielding effectiveness of the material is increased by increasing the loading of conductive fillers in the composite films respectively. Here's a variation in the thickness of the samples which is due to highly dispersed CNFs into the matrix and that thickness strongly correlates with the delay in the signal transmission shown in Figure below.

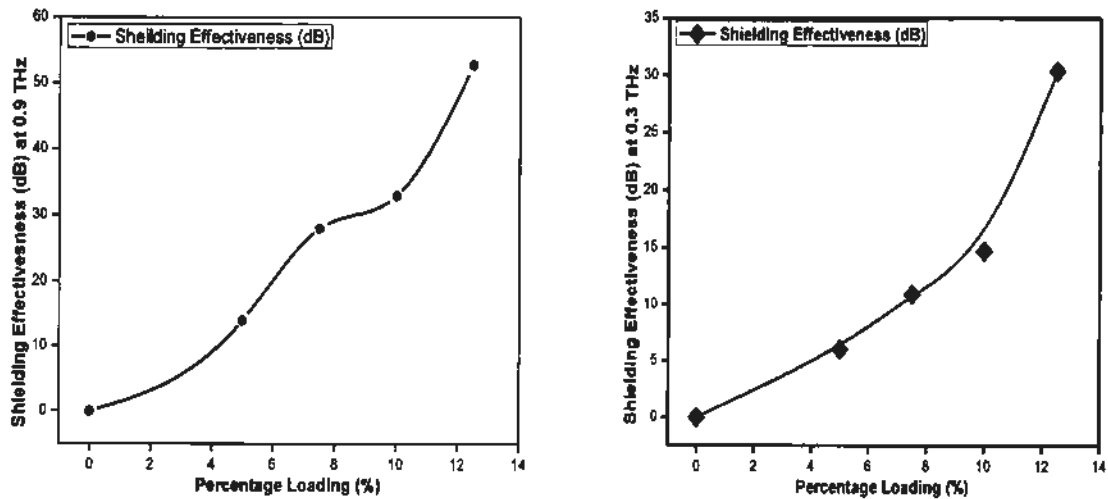
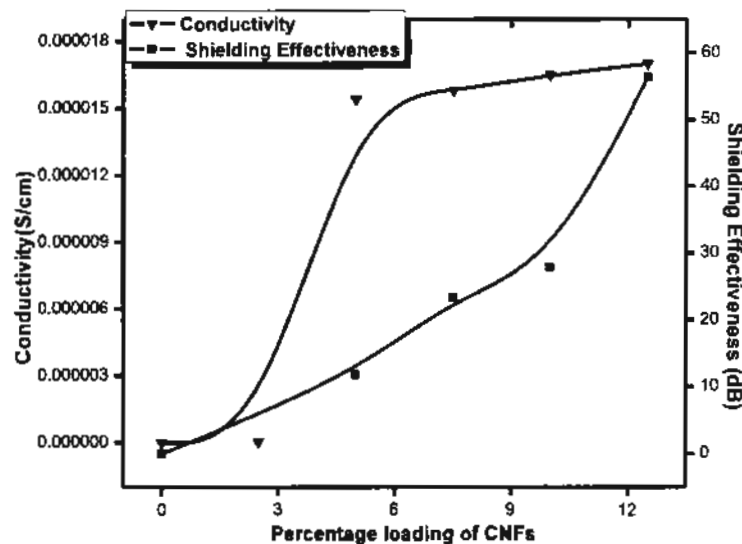


Figure 5-14: Shielding Effectiveness in THz frequency range 0.2-1.2 THz

The above figure indicates that the SE is based on the percentage loading of CNFs in a polymer matrix and frequency. As we increase the loading of CNFs in polymer matrix the SE is increasing [64]. Similarly, with increasing the frequency the SE increases. It is shown in Fig (a) & (b) at 0.3 THz frequency the SE at maximum loading is 30.4 dB and at 0.9 THz frequency the SE at maximum loading is 56.8 dB. It was concluded that the conductive fillers play an important role in materials shielding against EM radiations.

### Comparison b/w Electrical Conductivity & Shielding Effectiveness



*Figure 5-15: Electrical Conductivity VS. Shielding Effectiveness*

Figure 5-15 shows how shielding effectiveness correlates with electrical conductivity. As the conductivity is increased, the shielding effectiveness of the material also increases respectively. This result shows the dependence of shielding effectiveness of the conductivity of the material. It was concluded that the conductive filler plays important role in material shielding against EM radiation.



## **6 Conclusions and Future Recommendations**

### **6.1 Conclusions**

The aim of this dissertation was to develop an effective shielding material of polymer nanocomposite with conductive filler for suppression of electromagnetic radiation, while maintaining the light weight, volume efficient and flexible composite film. Comparison of experimental data with a pervious published research works to determine the several parameters affecting the shielding effectiveness. By analyzing the filler, matrix, and the composite formulation parameters, one can reach several conclusions. In this work, nanocomposite thin films of PMMA loaded with a range (0.00-12.50wt%) of CNFs have successfully been prepared by solvent evaporation method.

These composite films were found to be polycrystalline having well distributed CNFs in the PMMA matrix. A conductivity enhancement of the order of 6 has been observed with conductivity value from  $0.79 \times 10^{-10}$  S/cm to  $0.170 \times 10^{-4}$  S/cm in the sample having 12.50wt% of CNFs. SE value of 56.8dB has been evaluated in the nanocomposite films loaded with 12.50wt% of CNFs to that of Pure polymer was 0dB. SE is increased with increasing CNFs loading as well as it increased as frequency increased.

The formulation of polymer blend as the matrix and well distribution of conductive filler were responsible for significant shielding effectiveness through the composite film. Finding an optimum combination of polymer matrix with conductive filler for a given application is highly desirable. Highly conductive filler in insulating polymer matrix, results the superior strength and shielding. The shielding effectiveness depends on the loading of filler as the loading of CNFs is increased, the SE is increasing.

Shielding effectiveness also increased as frequency increased. This is ascribed to planar wave. At higher frequency, wavelength becomes smaller. Therefore, the wave cannot penetrate into the composite film as easy. The planar wave also depends upon the dielectric constant of composite material and sounding. The dielectric of free

space is less than conductive material. The dielectric constant is directly related to energy absorption, which makes shielding effectiveness increase with frequency.

A new research work needs to be developed the multilayer coating of composite film with significant thickness for enhancing shielding effectiveness.

## **Future Recommendations**

There are vast areas of exploring the applications of shielding the electromagnetic radiation by using of polymer nanocomposite materials. More research into these effects needs to be done. There are following recommendations suggested for future studies in this area.

For future work, make use of different conductive polymers as matrix. Use of different types of conductive fillers i.e. CNTs, iron oxides, metal flaks, coated fillers etc. By using different techniques and different materials, one can make nanocomposites films for shielding purposes. By picking different frequency ranges, we can get Shielding effectiveness in different bands. Highly conductive fillers can also be used for high SE with very low loading of fillers while maintaining the light weight, volume efficient and flexible nanocomposite films.

The conductive filler is currently used for their ability to produce conduction in insulating matrix, which is responsible for shielding the EMI. Further research is recommended in this area to make use of conductive polymer as matrix for better linking path with filler and achieve the good conductivity with less loading of filler, which is responsible for better shielding effectiveness at a very low loading of conductive fillers. That makes a composite film more flexible and volume efficient.

In order to make further improvement, different types of fillers should be used to understand which properties have influenced on shielding. Iron oxide, metal flakes, and coated fillers could be used. By studying the properties of fillers individually and make them use a polymer matrix, one could be able to develop a more sophisticated model for EMI shielding with heterogeneous filler.

## **References**

1. L.Olmedo, P. Hourquebie, and F. Jousse, "Handbook of Organic Conductive Molecules and Polymers" Chichester: 4 (1997) 367.
2. Li, N., Huang, Y., Du, F., He, X., Lin, X., Gao, H., Eklund, P. C. "Electromagnetic interference (EMI) shielding of single-walled carbon nanotube epoxy composites", *Nano letters*, 6 (2006) 1141.
3. Saini, P., Choudhary, V., Vijayan, N., & Kotnala, R. K. "Improved electromagnetic interference shielding response of poly (aniline)-coated fabrics containing dielectric and magnetic nanoparticles", *The Journal of Physical Chemistry C*, 116 (2012) 13403.
4. Reshi, H. A., Singh, A. P., Pillai, S., Yadav, R. S., Dhawan, S. K., & Shelke, V. "Nanostructured  $\text{La}_{0.7}\text{Sr}_{0.3}\text{MnO}_3$  compounds for effective electromagnetic interference shielding in the X-band frequency range", *Journal of Materials Chemistry C*, 3 (2015) 820.
5. Zhang, C. S., Ni, Q. Q., Fu, S. Y., & Kurashiki, K. "Electromagnetic interference shielding effect of nanocomposites with carbon nanotube and shape memory polymer", *Composites Science and Technology*, 67 (2007) 2973.
6. P.Chandrasekhar, *Conducting Polymers, "Fundamentals and Applications: A Practical Approach*, London: Kluwer Academic (1999) 330.
7. Strumpler R and G.-R. J., "Conducting polymer composites" *Journal of Electroceramics.* , 3 (1999) 329.
8. Al-Saleh, M. H., & Sundararaj, U. "Electromagnetic interference (EMI) shielding effectiveness of PP/PS polymer blends containing high structure carbon black", *Macromolecular Materials and Engineering*, 7 (2008) 621.
9. Bright Idea: The First Lasers. 2015  
<https://www.aip.org/history/exhibits/laser/sections/ravdevices.html>.
10. Bigg, D., "The effect of compounding on the conductive properties of EMI shielding compounds. *Advances in Polymer Technology*" 4 (1984) 255.
11. White, D., *EMI/EMC Handbook Series*, Don White Consultants. Inc., Germantown, MD, 4 (1971) 667.
12. Burrell, J. "Disruptive effects of electromagnetic interference on communication and electronic systems" (Doctoral dissertation, George Mason University) (2003).
13. Yang, S., Lozano, K., Lomeli, A., Foltz, H. D., & Jones, R. "Electromagnetic interference shielding effectiveness of carbon nanofiber/LCP composites." *Composites Part A: applied science and manufacturing*, 36, (2005), 691.
14. Wu, J., & Chung, D. D. L. "Improving colloidal graphite for electromagnetic interference shielding using 0.1  $\mu\text{m}$  diameter carbon filaments" *Carbon*, 41 (2003) 1313.
15. Chung, D. D. "Materials for electromagnetic interference shielding", *Journal of Materials Engineering and Performance*, 9 (2000) 350.
16. Osawa, Z., & Kuwabara, S. Thermal stability of the shielding effectiveness of composites to electromagnetic interference. Effects of matrix polymers and

## REFERENCES:

---

- surface treatment of fillers. *Polymer degradation and stability*, **35** no.1, (1992). 33.
17. Rosenow, M.W. and J. Bell, EMI shielding effectiveness of nickel coated carbon fiber as a long fiber thermoplastic concentrate. *Materials and Process Affordability: Keys to the Future.*, **43**, (1998) 854.
  18. Thostenson, E.T., C. Li, and T.-W. Chou, Nanocomposites in context. *Composites Science and Technology*, **65** no.3 (2005) 491.
  19. Fedullo, N., et al., Polymer-based nanocomposites: Overview, applications and perspectives. *Progress in organic coatings*, **58** no. (2007) 87.
  20. Aparna.A.R., V. Brahmajirao, and T.V.Karthikeyan., Review on Nano particle synthesis for usage in Nano-Composites for EMI shielding. *International Journal of Innovative Research in Science, Engineering and Technology.*, **2** (2013) 7391.
  21. Saini, P., et al., "Enhanced microwave absorption behavior of polyaniline-CNT/polystyrene blend in 12.4–18.0 GHz range", *Synthetic Metals*, **161** (2011) 1522.
  22. S. Iijima, " Highly strong and conductive carbon nanotube/cellulose composite paper" *Nature*. **354** (1991) 56.
  23. Ajayan and P.M., "Aligned Carbon Nanotube Arrays Formed by Cutting a Polymer Resin—Nanotube Composite", *Science*. **265** (1994) 1212.
  24. R. Saito, G. Dresselhaus, and M.S. Dresselhaus, *Physical Properties of Carbon Nanotubes*. 1999, London: Imperial College Press.
  25. C. A. Grimes, et al., *Chem. Phys. Lett.*, **319** (2000) 460.
  26. Files, B. S., & Mayeaux, B. M. "Carbon nanotubes" *Advanced materials & processes*, **156** (1999) 47.
  27. Ajayan, P. M., & Schadler, L. S. Carbon nanotube filled polymer nanocomposites. *Polymer Preprints(USA)*, **42** (2001) 35.
  28. Joo, J., & Epstein, A. J. "Electromagnetic radiation shielding by intrinsically conducting polymers." *Applied physics letters*, **65** (1994) 2278.
  29. Thomassin, J. M., Jérôme, C., Pardoën, T., Bailly, C., Huynen, I., & Detrembleur, C. "Polymer/carbon based composites as electromagnetic interference (EMI) shielding materials" *Materials Science and Engineering: R: Reports*, **74** (2013) 211.
  30. Gupta, A., & Choudhary, V. "Electromagnetic interference shielding behavior of poly (trimethylene terephthalate)/multi-walled carbon nanotube composites", *Composites Science and Technology*, **71** (2011) 1563.
  31. Imai, M., Akiyama, K., Tanaka, T., & Sano, E. "Highly strong and conductive carbon nanotube/cellulose composite paper", *Composites Science and Technology*, **70** (2010) 1564.
  32. Han, M. S., Lee, Y. K., Kim, W. N., Lee, H. S., Joo, J. S., Park, M., Park, C. R. "Effect of multi-walled carbon nanotube dispersion on the electrical, morphological and rheological properties of polycarbonate/multi-walled carbon nanotube composites" *Macromolecular research*, **17** (2009). 863.
  33. Mathur, R. B., Pande, S., Singh, B. P., & Dharmi, T. L. "Electrical and mechanical properties of multi-walled carbon nanotubes reinforced PMMA and PS composites" *Polymer Composites*, **29** (2008) 717.
  34. Huang, Y. L., Yuen, S. M., Ma, C. C. M., Chuang, C. Y., Yu, K. C., Teng, C. C., Weng, F. B. "Morphological, electrical, electromagnetic interference (EMI) shielding, and tribological properties of functionalized multi-walled

## REFERENCES:

---

- carbon nanotube/poly methyl methacrylate (PMMA) composites" *Composites Science and Technology*, **69** (2009) 1991.
35. Li, Y., Chen, C., Li, J. T., Zhang, S., Ni, Y., Cai, S., & Huang, J. "Enhanced dielectric constant for efficient electromagnetic shielding based on carbon-nanotube-added styrene acrylic emulsion based composite" *Nanoscale research letters*, **5** (2010), 1170.
  36. Li, Y., Chen, C., Zhang, S., Ni, Y., & Huang, J. "Electrical conductivity and electromagnetic interference shielding characteristics of multiwalled carbon nanotube filled polyacrylate composite films" *Applied Surface Science*, **254** (2008), 5766.
  37. Nguyen Thi Thanh, B., Phung Viet, T., Vu Thi, B., Nguyen Thanh, B., Dao Duy, T., Pham Duc, K., Nguyen Dinh, H. "The synergistic effect of bremsstrahlung photons and intense laser radiation on the structural properties of carbon nanotubes" **4** (2011) 165.
  38. Chen, I. H., Wang, C. C., & Chen, C. Y. "Fabrication and structural characterization of polyacrylonitrile and carbon nanofibers containing plasma-modified carbon nanotubes by electrospinning" *The Journal of Physical Chemistry C*, **32** (2010) 13532.
  39. Yang, Yonglai, et al. "Novel carbon nanotube– polystyrene foam composites for electromagnetic interference shielding." *Nano letters* **5** (2005) 2131.
  40. Das, Arindam, et al. "Superhydrophobic and conductive carbon nanofiber/PTFE composite coatings for EMI shielding." *Journal of colloid and interface science* **2** (2011) 311.
  41. Bose, S., et al., "Process optimization of ultrasonic spray coating of polymer films" *Langmuir*, **29** (2013) 6911.
  42. Perfetti, G., et al., "Relation between surface roughness of free films and process parameters in spray coating" *European Journal of Pharmaceutical Sciences*, **42** (2011) 262.
  43. Klug, H.P. and L.E. Alexander, "X-ray diffraction procedures" Wiley New York, **2** (2010) 1954:
  44. Warren, B.E., X-ray Diffraction. 1969: Courier Corporation.
  45. Deriving an informal interpretation of Bragg's Law [cited 2015 3/6/2015]; Available from: [http://www.xtal.iqfr.csic.es/Cristalografia/parte\\_05\\_5-en.html](http://www.xtal.iqfr.csic.es/Cristalografia/parte_05_5-en.html).
  46. Goebel, H. (1994). U.S. Patent No. 5,373,544. Washington, DC: U.S. Patent and Trademark Office.
  47. Leng, Y., *Materials characterization: "Introduction to microscopic and spectroscopic methods"*, John Wiley & Sons (2009).
  48. *Handbook Of Analytical Methods For Materials. Materials Evaluation and Engineering*, Inc (2001).
  49. M Joshi, A Bhattacharyya, and S.W. Ali, "Characterization techniques for nanotechnology applications in textile" *Indian Journal of Fibre and Textile Research*, **33** (2008) 304.
  50. Downes, A. and A. Elfick, "Raman spectroscopy and related techniques in biomedicine" *Sensors*, **10** (2010)1871.
  51. Bunaciu, A.A., H.Y. Aboul-Enein, and Ş. Fleschin, "Vibrational Spectroscopy in Clinical Analysis" *Applied Spectroscopy Reviews*, **50** (2015) 176.
  52. De Gelder, J., et al., "Reference database of Raman spectra of biological molecules" *Journal of Raman Spectroscopy*, **38** (2007) 1133.

## REFERENCES:

---

53. Li, N., et al., "Electromagnetic interference (EMI) shielding of single-walled carbon nanotube epoxy composites" *Nano letters*, **6** (2006) 1141.
54. David Halliday, Robert Resnick, and J. Walker, *FUNDAMENTALS OF PHYSICS*. 9th ed., United States: John Wiley & Sons, Inc.
55. Study the temperature dependence of resistance of a semiconductor (Four probe method) (2012); Available from: [www.sardarsinghsir.com](http://www.sardarsinghsir.com).
56. Naftaly, M. and R.E. Miles, Terahertz time-domain spectroscopy for material characterization. *PROCEEDINGS-IEEE*, 2007. **95**(8): p. 1658.
57. Hussain, B., et al., "Measurement of thickness and refractive index using femtosecond and terahertz pulses" *Laser Physics Letters*, **10** (2013) 055301.
58. Schürmann, U., et al., "Controlled syntheses of Ag–polytetrafluoroethylene nanocomposite thin films by co-sputtering from two magnetron sources" *Nanotechnology*, **16** (2005) 1078.
59. Sharma, M., K. Sharma, and S. Bose, "Segmental relaxations and crystallization-induced phase separation in PVDF/PMMA blends in the presence of surface-functionalized multiwall carbon nanotubes" *The Journal of Physical Chemistry B*, **117** (2013) 8589.
60. Baker, A.M., et al., "Nafion membranes reinforced with magnetically controlled Fe<sub>3</sub>O<sub>4</sub>-MWCNTs for PEMFCs" *Journal of Materials Chemistry*, **22** (2012) 14008.
61. Park, S.J., et al., "Synthesis and Dispersion Characteristics of Multi-Walled Carbon Nanotube Composites with Poly (methyl methacrylate) Prepared by In-Situ Bulk Polymerization" *Macromolecular Rapid Communications*, **24** (2003) 1070.
62. Schürmann, U., et al., "Controlled syntheses of Ag–polytetrafluoroethylene nanocomposite thin films by co-sputtering from two magnetron sources" *Nanotechnology*, **16** (2005) 1078.
63. Polley, D., et al., Polarizing effect of aligned nanoparticles in terahertz frequency region. *Optics letters*, **38** (2013) 2754.
64. Polley, D., A. Barman, and R.K. Mitra, "EMI shielding and conductivity of carbon nanotube-polymer composites at terahertz frequency" *Optics letters*, **39** (2014) 1541.